


## REVIEW

[View Article Online](#)  
[View Journal](#) | [View Issue](#)Cite this: *RSC Adv.*, 2018, 8, 20952

# Stability of organometal halide perovskite solar cells and role of HTMs: recent developments and future directions

Ehsan Raza,<sup>a</sup> Fakhra Aziz<sup>b</sup> and Zubair Ahmad \*<sup>c</sup>

Perovskite solar cells (PSCs) have recently emerged as one of the most exciting fields of research of our time, and the World Economic Forum in 2016 recognized them as one of the top 10 technologies in 2016. With 22.7% power conversion efficiency, PSCs are poised to revolutionize the way power is produced, stored and consumed. However, the widespread use of PSCs requires addressing the stability issue. Therefore, it is now time to focus on the critical step *i.e.* stability under the operating conditions for the development of a sustainable and durable PV technology based on PSCs. In order to improve the stability of PSCs, hole transport materials (HTMs) have been considered as the paramount components. This is due to the fact that most of the organic HTMs possess a hygroscopic and acidic nature that leads to poor stability of the PSCs. This article reviews briefly but comprehensively the environmental stability issues of PSCs, fundamentals, strategies for improvement, the role of HTMs towards stability and various types of HTMs. Also the environmental parameters affecting the performance of perovskite solar cells including temperature, moisture and light soaking environment have been considered.

Received 23rd April 2018

Accepted 26th May 2018

DOI: 10.1039/c8ra03477j

[rsc.li/rsc-advances](http://rsc.li/rsc-advances)

## 1. Recent advancement in PSCs

For the first time, in 2006, Miyasaka and co-workers<sup>1–3</sup> reported the potential use of perovskite as a light absorbing material (*e.g.* methylammonium lead bromine  $\text{CH}_3\text{NH}_3\text{PbBr}_3$ ) in dye sensitized solar cells and stated the power conversation efficiency (PCE) as 2.2%.<sup>3</sup> In 2009, they replaced bromine with iodine and demonstrated a slight increase in the efficiency *i.e.* 3.8%<sup>4</sup> (all devices were unstable). Later, in 2011, Park and colleagues fabricated perovskite based highly efficient quantum-dot (QD) sensitized solar cells and reported a PCE of 6.5%.<sup>5</sup> Despite a considerable leap in power conversion efficiency (PCE),<sup>6</sup> QDs tend to dissolve in the redox electrolyte. Hence, Park and Gratzel introduced the first solid-state mesoscopic solar cell based on perovskite nanocrystals, mesoporous  $\text{TiO}_2$  layers and spiro-MeOTAD as hole transporting material (HTM) and boosted the PCE to 9.7%<sup>7</sup> along with long term stability ( $\sim$  for 500 h). Afterwards, Snaith and co-workers introduced meso-superstructured solar cells (MSSCs), in which they replaced non conducting  $\text{Al}_2\text{O}_3$  with mesoporous conducting n-type  $\text{TiO}_2$  and reported a PCE of 10.9%.<sup>8</sup> An improvement in efficiency to 12% was reported after the combined efforts of M. K.

Nazeeruddin, Gratzel, Seok and co-workers.<sup>9</sup> In their work, they introduced a layered sandwich type structure in which three dimensional nanocomposites of mesoporous (mp)- $\text{TiO}_2$ , with methylammonium lead triiodide  $\text{CH}_3\text{NH}_3\text{PbI}_3$  as light harvester and polymeric hole transport materials were used. Seok's group further improved efficiency to 12.3% with the same structure but mixed halide  $\text{CH}_3\text{NH}_3\text{PbI}_{3-x}\text{Br}_x$  perovskites.<sup>10</sup> For the first time, Huckaba *et al.*<sup>11</sup> studied low cost  $\text{TiS}_2$  p-type contact material (30 times lower in price as compared to spiro-OMeTAD) as HTM, synthesized by a simple two step hot injection method and reported 13.5% PCE. In early 2013 during the European Materials Research Symposium, two groups reported efficiencies above 15%.<sup>12</sup> Gratzel's group reported 15% by using mesoporous  $\text{TiO}_2$  and two-step sequential of lead iodide ( $\text{PbI}_2$ ) with improved morphology. While Snaith's group reported 15.4% efficiency with better morphology.<sup>1</sup> They used simple structure of  $\text{CH}_3\text{NH}_3\text{PbI}_{3-x}\text{Cl}_x$  deposited by two-source thermal evaporation method. M. K. Nazeeruddin and group demonstrated 15.4% PCE using newly synthesized benzothiadiazole substituted derivatives, 4-(3,5-bis(trifluoromethyl)phenyl)-7-(5'-hexyl-[2,2'-bithiophen]-5-yl)benzo[c][1,2,5]thiadiazole (CF-BTz-ThR) as HTM and aligned  $\text{TiO}_2$  nano bundles ( $\text{TiO}_2$  NBs) as ETL and fabricated high performance  $\text{CH}_3\text{NH}_3\text{PbI}_3$  PSC.<sup>13</sup> M. K. Nazeeruddin *et al.*<sup>14</sup> investigated low-temperature solution processable deoxyribose nucleic acid (DNA)-hexydecyl trimethyl ammonium chloride (CTMA) as HTM and (6,6)-phenyl C61-butyric acid methyl ester (PCBM) as electron-acceptor layer in inverted p-i-n configuration based perovskite solar cells and reported 15.86% PCE. Late in 2013, Seok and co-workers used

<sup>a</sup>Department of Electronics, Faculty of Physical and Numerical Sciences, University of Peshawar, Peshawar 25120, Pakistan<sup>b</sup>Department of Electronics, Jinnah College for Women, University of Peshawar, Peshawar 25120, Pakistan<sup>c</sup>Center for Advanced Materials (CAM), Qatar University, 2713 Doha, Qatar. E-mail: [zubairtarar@qu.edu.qa](mailto:zubairtarar@qu.edu.qa)

$\text{CH}_3\text{NH}_3\text{Pb}(\text{I}_{1-x}\text{Br}_x)_3$  as light harvester and poly(triarylamine) as HTM and gained 16.2%<sup>15</sup> PCE. C. K. Teak and fellows studied easily accessible zinc phthalocyanines including tetra-*tert*-butyl ZnPc, tetra-5-hexyl-2,2'-bisthiophene-substituted zinc phthalocyanines (ZnPcs) and tetra-5-hexylthiophene- as hole transporting materials in mixed ion perovskite  $[\text{FAPbI}_3]_{0.85}[\text{MAPbBr}_3]_{0.15}$  based solar cells and achieved PCEs of 13.3%, 15.5% and 17.5% for TB-ZnPc, HBT-ZnPc and HT-ZnPc, respectively.<sup>16</sup> Their work paved the way for solution processed ZnPc derivatives as stable and cost effective hole transport materials for wide scale, efficient and inexpensive energy production applications. Earlier in 2014, again Seok and group members reported an efficiency of 17.9%.<sup>17</sup> P. Sanghyun *et al.* designed star shaped D- $\pi$ -A type HTMs including a rigid quinolizino acridine (FA-CN) and a flexible triphenylamine (TPA-CN) as central unit and donor part, alkyl-substituted terthiophene as a conjugated bridge and malononitrile as an electron acceptor. Dopant free FA-CN and TPA-CN based devices exhibited PCEs of 18.9% and 17.5%, respectively, under AM 1.5 illuminations.<sup>18</sup> M. K. Nazeeruddin and fellows demonstrated 19% PCE with stabilized performance for 1000 h under continuous light illumination by adding large organic cation guanidinium (Gua) into  $\text{MAPbI}_3$ .<sup>19</sup> For the first time, M. K. Nazeeruddin and fellows introduced a simple and highly reproducible approach to obtain highly efficient hybrid perovskite solar cells by combining 10% of formamidinium (FA) with methylammonium lead iodide ( $\text{MAPbI}_3$ ) and reported 20.2% PCE.<sup>20</sup> M. K. Nazeeruddin and group studied a combination of triple Cs/MA/FA cation by adding a small amount of inorganic cesium (Cs) and achieved highly efficient PSCs with stabilized PCEs of 21.1% and outputs at 18% under operational conditions after 250 hours.<sup>21</sup> Their work opened the doors for other scientists and researchers to explore alkali metals like K, Li, Na and Rb as cations for perovskites.<sup>21</sup> Some researchers and scientists from Korea reported 22.1% PCE by introducing additional iodide ions into the organic cation solution.<sup>22</sup> Recently in 2017, a team from Korean Research Institute of Chemical Technology (KRICT) developed a perovskite based solar battery cells and boosted the power conversion efficiency upto 22.7%<sup>18</sup> (the highest PCE on record so far).

Ye *et al.*<sup>23</sup> and fellows performed n-type doping of bis(1-[3-(methoxycarbonyl)propyl]-1-phenyl)-[6,6]C62 (Bis-PCBM) with decamethylcobaltocene (DMC). The device exhibited smooth surface morphology, good solvent resistance and improved device stability. The maximum PCE of 20.14% was reported.<sup>23</sup> M. Qian and co-workers examined the device performance by anode modification in which they doped silver nano-particles (Ag NPs) with poly(3,4-ethylenedioxythiophene):poly(4-styrenesulfonate) (PEDOT:PSS) and cathode interfacial modification by adding a solution processed bathophenanthroline (sBphen) in  $\text{CH}_3\text{NH}_3\text{PbI}_{3-x}\text{Cl}_x$  based PSC. Using this approach, they exhibited PCE as high as 15.75%.<sup>24</sup> Z. Wang and fellows demonstrated solution processed PEDOT:PSS- $\text{GeO}_2$  composite films as a hole transport layer in planar structure PSC. The device exhibited PCE of

15.15% and fill factor (FF) of 74%.<sup>25</sup> Zheng *et al.*<sup>26</sup> studied various solution processed interfacial layers of transition metal oxides (TMOs) including molybdenum oxide ( $\text{MoO}_3$ ), vanadium oxide ( $\text{V}_2\text{O}_5$ ), germanium dioxide ( $\text{GeO}_2$ ) and chromium trioxide ( $\text{CrO}_3$ ). Among these  $\text{V}_2\text{O}_5$  film showed highest work function (5.2 eV) with best hydrophobic property at a contact angle of 72.2°.  $\text{V}_2\text{O}_5$  based organic solar cells (OSCs) and perovskite solar cells (PSCs) exhibited PCEs of 8.36% and 14.13%, respectively. When used as a composite with PEDOT:PSS, the PEDOT:PSS: $\text{V}_2\text{O}_5$  based PSCs showed improved device performance with PCE of 18.03%. Wang *et al.*<sup>27</sup> developed an efficient and stable hole transport material tetra-fluorotetracyanoquinodimethane (F4-TCNQ)-doped copper phthalocyanine-3,4',4'',4'''-tetra-sulfonated acid tetra sodium salt (TS-CuPc) in planar structure PSCs by solution processing. Using TS-CuPc:F4-TCNQ as the hole transporting material, they achieved PCEs of 16.14% for p-i-n structure and 20.16% for n-i-p structure, respectively. Li *et al.*<sup>28</sup> developed copper salts (cuprous thiocyanate ( $\text{CuSCN}$ ) or cuprous iodide ( $\text{CuI}$ )) doped spiro-OMeTAD based solution processed, stable hole transport materials. By p-doping they improved device performance and enhanced the PCE from 14.82% to 18.02%. Z. Wang and co-workers developed a thin perylene underlayer using solution processed method. The multifunctional perylene improved the overall device performance and significantly enhanced the PCE from 12.67% to 17.06%.<sup>29</sup> Such rapid improvement in less than 5 years suggests that organometal halide perovskites are indeed a new class of solar absorber. Fig. 1 provides the general view on the efficiency trends of perovskite solar cells from 2009 to 2017.

## 2. Stability of perovskite solar cell

Recently, over the past few years, hybrid organic-inorganic halide perovskites have been developed as potential candidates for photovoltaic applications. Device instability and degradation under ambient conditions restrict them for commercialization. Stability is currently one of the most investigated topics in PSCs. The devices that exhibited higher efficiencies comparable to silicon-based devices were degraded quickly. To improve the device stability, a basic understanding of the stability should be acquired. Factors that have an impact on the stability of perovskites have been explored. Normally, degradation in perovskites is caused by air (moisture & oxygen), UV-light, elevated temperature and chemical degradation as shown in Fig. 2. Here below, the stability has been categorized into two types which includes chemical stability and thermal stability.

### 2.1. Chemical stability

The chemical stability of perovskite solar cells refers to a series of chemical reactions under various conditions and atmospheres. The main factors that affect chemical stability in PSCs are oxygen, moisture and UV light. Many reports regarding aforementioned factors have addressed the degradation issues in PSCs. During the process of fabrication, testing and assembling, moisture and oxygen might have direct influence on the



## Efficiency Trends &amp; Associated Timeline

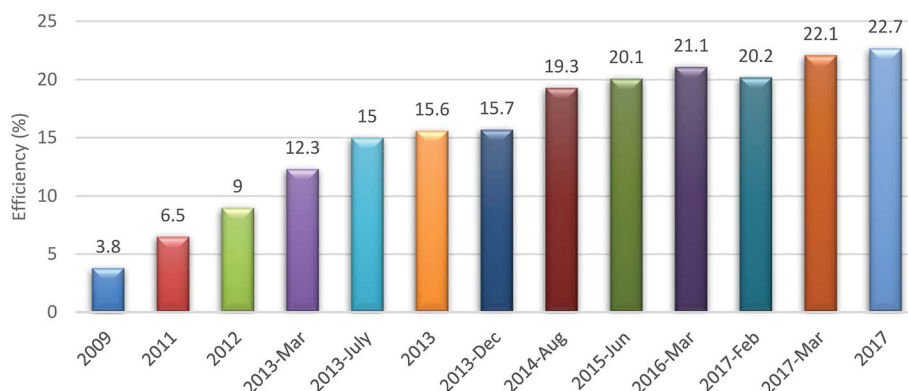
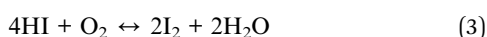
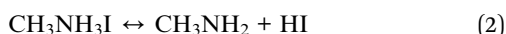


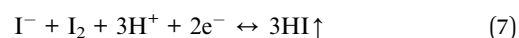
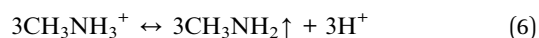
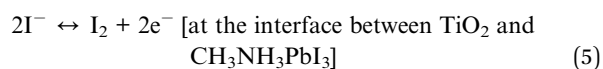
Fig. 1 General view on the efficiency trends of perovskite solar cells from 2009 to 2017.

stability during the reaction process.<sup>30,31</sup> Niu *et al.*<sup>32</sup> studied the moisture effect on  $\text{CH}_3\text{NH}_3\text{PbI}_3$  perovskite. They suggested that  $\text{CH}_3\text{NH}_3\text{PbI}_3$  is highly sensitive to moisture and gets easily degraded.<sup>31,32</sup> They presented degradation mechanism as mentioned below in eqn (1)–(4). They reported that in the presence of moisture  $\text{CH}_3\text{NH}_3\text{PbI}_3$  decomposes into  $\text{CH}_3\text{NH}_3\text{I}$  and  $\text{PbI}_2$  as shown in reaction (1). In reaction (2),  $\text{CH}_3\text{NH}_3\text{I}$  further decomposes into  $\text{CH}_3\text{NH}_2$  and  $\text{HI}$ .  $\text{HI}$  can react in the following two ways. One way is using redox reaction method in the presence of oxygen (3). The second is photochemical method in which,  $\text{HI}$  breaks down into  $\text{H}_2$  and  $\text{I}_2$  under UV radiation as shown in reaction (4).



A similar impression was reported by Walsh *et al.*<sup>19</sup> that  $\text{MAPbI}_3$  is partially decomposed on exposure to moisture<sup>19</sup>. They proposed that a single molecule in  $\text{H}_2\text{O}$  known as Lewis base, reacts with  $\text{MAPbI}_3$  and extracts one proton from ammonium leading to intermediates. Furthermore, these

intermediates may decompose into  $\text{HI}$ ,  $\text{CH}_3\text{NH}_2$  and solid  $\text{PbI}_2$ . Gong *et al.*<sup>33</sup> studied the degradation phenomena in perovskite solar cells. They reported DR3TBDTT as hydrophobic hole transporting material (HTM) with improved stability suggesting DR3TBDTT as moisture resistant potential candidate.<sup>33</sup> Aristidou and co-workers studied the combined effect of light and oxygen on the stability of  $\text{CH}_3\text{NH}_3\text{PbI}_3$  perovskite. They observed that the reaction between superoxide ( $\text{O}_2^-$ ) and methylammonium moiety of the perovskite layer turned out to be the cause of degradation in  $\text{CH}_3\text{NH}_3\text{PbI}_3$  perovskite.<sup>34</sup> Snaith *et al.*<sup>35</sup> studied the stability in  $\text{TiO}_2$ -sensitized meso-superstructured solar cell (MSSC) under UV radiation for the first time. They identified the instability due to light induced desorption of oxygen which is adsorbed on the surface of mesoporous  $\text{TiO}_2$ . The instability issue was resolved by implementing an insulating mesoporous  $\text{Al}_2\text{O}_3$  scaffold as a substitute of n-type mesoporous  $\text{TiO}_2$ . The  $\text{Al}_2\text{O}_3$  based MSSC showed improved stability and stable photo currents under continuous full spectrum of sunlight over a period of 1,000 h.<sup>35</sup> Hitoshi *et al.*<sup>36</sup> studied the stability of  $\text{CH}_3\text{NH}_3\text{PbI}_3$  perovskite without encapsulation under one sun irradiation (AM 1.5). They observed that the decomposition appeared at the interface between  $\text{TiO}_2$  and  $\text{CH}_3\text{NH}_3\text{PbI}_3$ . For this they proposed possible reaction at the interface between  $\text{TiO}_2$  and  $\text{CH}_3\text{NH}_3\text{PbI}_3$  as given in eqn (5)–(7):



As far as the stability under illumination is concerned, a study is conducted by adding  $\text{Sb}_2\text{S}_3$  at the interface of  $\text{TiO}_2$  and  $\text{CH}_3\text{NH}_3\text{PbI}_3$ . With addition of  $\text{Sb}_2\text{S}_3$  as a surface blocking layer, the stability of  $\text{CH}_3\text{NH}_3\text{PbI}_3$  was significantly improved.<sup>36</sup> Komarala *et al.*<sup>37</sup> demonstrated the UV degradation in  $\text{TiO}_2$  based  $\text{CH}_3\text{NH}_3\text{PbI}_3$  using down-shifting (DS)  $\text{YVO}_4:\text{Eu}^{3+}$  nanophosphor layer. The europium ( $\text{Eu}^{3+}$ ) doped yttrium vanadate ( $\text{YVO}_4$ ) has a specific 4f electronic structure. This material

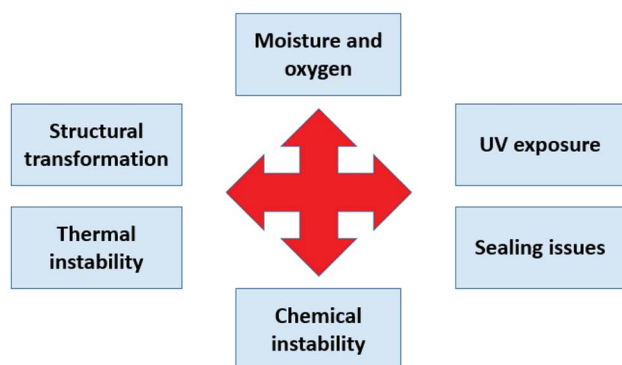


Fig. 2 Various factors which affect the stability in PSCs.



converts absorbed UV light into visible light which is then absorbed by  $\text{CH}_3\text{NH}_3\text{PbI}_3$ . Using this approach, they achieved ~8.5% enhancement in the photocurrent and improved stability of PSC under UV light exposure.

## 2.2. Thermal stability

According to the International Standards IEC 61646, at 85 °C long term stability is required to compete with silicon-based technology. Several factors affect thermal stability in perovskite devices such as intrinsic temperature (due to perovskite material itself), electrodes degradation and charge transporting layers *i.e.* hole transport materials (HTM) and electron transport materials (ETM) degradation. Gratzel *et al.*<sup>38</sup> examined the thermal behavior of the perovskite materials and analyzed thermal properties of their individual components. They observed the tetragonal to cubic phase transition in  $\text{PbI}_2$  precursor based perovskite which might affect thermal stability in perovskite. Pisoni *et al.*<sup>39</sup> studied the thermal conductive properties of  $\text{MAPbI}_3$ . In their experiments, large single crystals and polycrystalline samples showed very low thermal conductivity. Such low thermal conductivity could not allow light deposited heat to spread out quickly; this may cause mechanical stress and affect the performance of photovoltaic device. Snaith *et al.*<sup>40</sup> investigated thermal and moisture stability in perovskites. They employed a new class of hole transporting material polymer-functionalized single-walled carbon nanotubes (SWNTs) embedded in an inert polymer matrix and achieved thermal stability. Conings *et al.*<sup>41</sup> explored the intrinsic instability of perovskite material during heating at 85 °C. They reported the soft matter nature of perovskite layer by investigating morphological, electrical, chemical and optical characteristics of this new class of material. This experiment was performed in pure dry  $\text{N}_2$ , pure dry  $\text{O}_2$  and at ambient atmosphere with 50% relative humidity for 24 h in the dark.<sup>41</sup> Their results revealed that degradation starts at 85 °C, and its rate is reliant on surrounding atmosphere.

Misra and co-workers demonstrated degradation in encapsulated  $\text{MAPbI}_3$ . They observed no degradation when  $\text{MAPbI}_3$  was exposed to 1 suns (1 sun = 100 mW cm<sup>-2</sup>) at 25 °C for 60 minutes, while  $\text{MAPbI}_3$  started degrading when the temperature rose from room temperature to 45–55 °C.<sup>42</sup> N. G. Philippe *et al.*<sup>43–45</sup> investigated thermal stability by studying the ratios of I/Pb and N/Pb using hard X-ray photoelectron spectroscopy (HAXPES). The measurements were performed at room temperature, 100 and 200 °C for 20 minutes. As observed,  $\text{MAPbI}_3$  started to decompose into  $\text{PbI}_2$  [eqn (8)] with increase in temperature from room temperature to 100 °C and then to 200 °C. The estimated I/Pb and N/Pb ratios gained from HAXPES results, revealed that  $\text{MAPbI}_3$  to  $\text{PbI}_2$  ratio modified from 85 : 15 to 70 : 30 and to 0 : 100 respectively.<sup>43</sup>



Park *et al.*<sup>46</sup> reported a good thermal stability in  $\text{FAPbI}_3$  perovskite at an annealing temperature of 25 °C for 15 min. Similarly, Zhao *et al.*<sup>47</sup> demonstrated excellent thermal stability in  $\text{FAPbI}_3$  perovskite annealed at 160 °C for 80 min. Jin

*et al.*<sup>48</sup> proved that  $\text{FAPbI}_3$  is more thermally stable as compared to  $\text{MAPbI}_3$  or any other perovskite.<sup>49</sup> Han *et al.*<sup>50</sup> introduced tetrathiafulvalene derivative (TTF-1) as a hole transporting material (HTM) into PSCs. They achieved 11.03% PCE with improved stability as compared to spiro-OMeTAD (PCE ~ 11.04%). Meng *et al.*<sup>51</sup> revealed stable perovskite device structure with no hole transporting layer (HTL) and achieved PCE of 10.5%. Similarly, Conings *et al.*<sup>41</sup> and yang and co-workers reported thermal instability due to electron transporting layers *i.e.*  $\text{ZnO}$  and  $\text{TiO}_2$ .<sup>41,52</sup>

## 3. Strategies for improving stability

Several strategies have been addressed in the literature that can be adopted to improve stability issues in PSCs.

### 3.1. Modification in perovskite structure

One of the proposed strategies to improve stability is to tune  $\text{ABX}_3$  structure. Here A is a cation, B is a divalent metal ion and X is a halide. Seok *et al.*<sup>10</sup> have demonstrated an improved stability against moisture by controllable tuning of halide composition. Thiocyanate (SCN) group is a class of stable pseudohalogen having comparable properties of halogen. They can be used to tune the X halide composition to achieve best device stability.  $\text{SCN}^-$  has similar ionic radius as compared to  $\text{I}^-$ . Y. Chen and co-workers introduced a planar cell structure using  $\text{MAPbI}_{3-x}(\text{SCN})_x$  and reported good device stability with remarkably high reproducibility.<sup>53</sup> Without encapsulation,  $\text{MAPbI}_{3-x}(\text{SCN})_x$  retained 86.7% of its average efficiency at 70% RH for over 500 h, while  $\text{MAPbI}_3$  lost 40% of its original efficiency.<sup>54</sup>

Few research groups proposed routes to improve stability by tuning methylammonium as a cation with inorganic. Fully inorganic cesium-based perovskite has gained interest due to its potential of tolerating elevated temperatures.  $\text{CsPbX}_3$  based perovskites have demonstrated outstanding thermal stability. Furthermore, cesium cation can also stabilize the  $\text{FAPbI}_3$  crystal structure. Lee *et al.*<sup>55</sup> reported that cesium not only increases the efficiency *via* stabilization of black  $\text{FAPbI}_3$  perovskite phase but also improves film stability under light illumination and humidity environment. S. I. Seok's group demonstrated that under humid environment the stability of perovskite can be significantly enhanced by doping bromide with  $\text{MAPbI}_3$ .<sup>31,56</sup> They prepared (MPSC) devices using mixed halide perovskite  $\text{MAPb}(\text{I}_{1-x}\text{Br}_x)_3$ . To test the stability, the un-encapsulated devices were exposed to controlled humidity under ambient conditions. At 35% humidity, all devices exhibited no significant degradation in PCE. But when the humidity increased to 55%,  $\text{MAPb}(\text{I}_{0.8}\text{Br}_{0.2})_3$  and  $\text{MAPb}(\text{I}_{0.71}\text{Br}_{0.29})_3$  based devices showed good stability. On the other hand,  $\text{MAPbI}_3$  and  $\text{MAPb}(\text{I}_{0.94}\text{Br}_{0.06})_3$  based devices degraded rapidly. The devices based on  $\text{MAPb}(\text{I}_{1-x}\text{Br}_x)_3$  ( $x \geq 0.2$ ) exhibited enhanced stability under high humid environment due to compact and stable crystal structure.



### 3.2. Addition of filters/thin layers

Another approach to increase stability of the perovskite devices against UV light and moisture is the addition of a very thin layer between the perovskite and hole transport layers or electron extracting layers. Several hydrophobic layers have been introduced as moisture barriers between the perovskite layers and spiro-OMeTAD. The purpose of these layers is to block any moisture diffusion through the hole transport layers to prevent device degradation. The layers should be thin enough to allow charge transfer and thick enough to block moisture ingress. An ultra-thin layer of  $\text{Al}_2\text{O}_3$  was deposited between perovskite absorber and spiro-OMeTAD using atomic layer deposition (ALD). The device exhibited improved stability with 90% of the initial value at 50% RH for 24 hours without illumination. Guarnera *et al.*<sup>57</sup> reported improved device performance and stability by introducing a spin-coated layer of alumina nanoparticles between the perovskite layer and spiro-OMeTAD. Ito *et al.*<sup>36</sup> reported improved device stability under illumination by employing  $\text{Sb}_2\text{S}_3$  as a buffer layer between perovskite absorber and  $\text{TiO}_2$ . Li and co-workers stabilized the perovskite device by inserting a layer of CsBr between the perovskite and  $\text{TiO}_2$ .<sup>58</sup> Pathak *et al.*<sup>59</sup> developed Al-doped  $\text{TiO}_2$  and reported enhanced device stability and performance under full light exposure. Besides improved device stability, Al-doping has negative impact on charge extraction efficiency that results in a reduced photocurrent. To overcome this issue, neodymium (Nd) doping was introduced instead of Al doping. Nd-doped mesoporous  $\text{TiO}_2$  based devices demonstrated steady state efficiency of 18.2% with improved stability as compared to their undoped counterparts. In order to improve the device photo-stability, Zheng and co-workers completely replaced  $\text{TiO}_2$  with CdS as an n-type layer. After continuous exposure of light for 12 h, CdS based devices retained more than 90% of their initial efficiency, while  $\text{TiO}_2$  based devices experienced a decrease in their efficiency from 15.4 to 3.1%.<sup>60</sup>

To solve the stability issues for perovskite solar cells, a novel interface engineering approach was introduced by J. Chen and group members. In which they developed a versatile ultrathin 2D perovskite  $(5\text{-AVA})_2\text{PbI}_4$  ( $5\text{-AVA} = 5\text{-ammoniumvaleric acid}$ ) passivation layer at back contact between perovskite and CuSCN interface. By using back contact interface engineering, they achieved improved device performance along with photo and moisture stability.<sup>61</sup>

## 4. Role of HTM in stability

The HTMs are the major components of the PSCs which have much effect on the stability of PSCs. Stability depends on hydrophobic property and morphology of the HTM as well as the interface between HTM and perovskite layer. Organic HTMs are used in the most efficient perovskite solar cells. Hole transportation and retardation of charge recombination are their main function. So far, HTMs in perovskite solar cells mainly involve nitrogen-based donors such as 2,2',7,7'-tetrakis-(*N,N*-di-*p*-methoxyphenylamine)-9,9'-spiro-bifluorene (spiro-OMeTAD), poly-(triarylamine) (PTAA), and so on. Due to the

triangular pyramid configuration of  $\text{sp}^3$  hybridization of nitrogen atom, large intermolecular distances are present in the structure. As a result, they suffer from low hole mobility, low conductivity, or both, in their pristine form. Therefore, "redox active" p-type dopants, such as Li-bis(trifluoromethanesulfonyl) imide (Li-TFSI), have been commonly adopted to increase conductivity and thereby improve cell performance. However, such dopants have aggravated cell performance degradation because of their tendency to become liquid or to absorb moisture from air and get dissolved in the moisture. J. Liu *et al.*<sup>50</sup> used tetrathiafulvalene derivative (TTF-1) as a hole transport material (HTM) in a perovskite solar cell. The HTM did not use any dopant and resulted in the stability better than the one that uses spiro-OMeTAD, a p-type dopant.

For instance, M. K. Nazeeruddin and co-workers reported molecularly engineered star-shaped D- $\pi$ -A dopant free hole transport materials comprising rigid quinolizino acridine (FA-CN) and a flexible triphenylamine (TPA-CN). By this approach, they observed improved device efficiency and significantly enhanced stability as compared to doped spiro-OMeTAD under light soaking ( $100 \text{ mW cm}^{-2}$ ) conditions.<sup>62</sup> In an atom or atomic lattice, electron hole or hole is the absence of electron at a position where an electron could exist. For example, helium has two electrons in its atom, if an electron leaves helium, an electron hole is created. This also makes the helium atom positively charged. In metal, electrons and electron holes move in a similar way. In an electric field, the movement of holes slows down and results in slow performance of the electronic device. Further, F. Zhang and fellows synthesized and characterized two novel thiophene based HTMs, Z25 and Z26 and demonstrated a simple strategy by adding double bonds to the structure of hole transporting layers. This double bonding benefits hole mobility in Z26 based device which improves PCE to 20.1% and the device was more stable than Z25 and spiro-OMeTAD based devices.<sup>63</sup>

## 5. Hole transport materials (HTMs)

Solid state hole transport materials can be categorized into three main classes: organic, inorganic and hybrid. Table 1 provides a close look on the HTMs with their efficiencies and stabilities. Each type has different pros and cons, which will be discussed in the following sections.

### 5.1. Organic hole transport materials

Organic hole transport materials can be further categorized into small molecule HTMs and polymeric HTMs.

**5.1.1. Small molecule HTMs.** Low molecular weight organic materials are economical, simple to synthesize, easy to modify and possess solution processable nature.<sup>81</sup> This section review summarizes the research on small molecule HTMs used in standardized PSCs device structures. Spiro-OMeTAD (Fig. 3) is one of the most widely used organic small molecular HTMs and has produced highly efficient devices.<sup>81</sup> The problem with spiro-OMeTAD is its cost and poor hole mobility. To overcome these factors many HTMs have been introduced with almost



Table 1 Types of HTMs along their efficiencies and stability

Name	Efficiency	Stability	References
Spiro-OMeTAD	20.6%	—	—
P3HT	20%	800 h	64
Z25	16.9	Higher than spiro-OMeTAD (300 h)	63
Z26	20.1	Higher than spiro-OMeTAD (800 h)	63
DBTP	18.09	Higher than spiro-OMeTAD (81% retention after 792 h or 33 days)	65
TTA	16.7	Tested for 300 hours	66
SYN1	11.4	Outclass performance than spiro-OMeTAD based devices (value not mentioned)	67
PARA1	13.1	Outclass performance than spiro-OMeTAD based devices (value not mentioned)	67
TPA-ZnPC	13.65	Higher than spiro-OMeTAD (value not mentioned)	68
Q221	10.37	200 h	69
Q222	8.87	200 h	69
ZnPcNO <sub>2</sub> -OPh	14.35	Higher than spiro-OMeTAD (tested for 33 days, PCE decreased to 4%)	70
CuPcNO <sub>2</sub> -OPh	12.72	Higher than spiro-OMeTAD (tested for 33 days, PCE decreased to 18%)	70
Ag: NiOx	16.86	Higher than organic HTM (tested for 30 days, PCE mentioned over 80%)	71
BPNS	16.4	Lower than spiro-OMeTAD	72
PEDOT:PSS	20	Higher stability than pristine PEDOT:PSS based HTM	73
MoO <sub>3</sub>	15.8	Shows high stability in moisture	74
Triazatruxene	15	Hydrophobic in nature (value not mentioned)	75
PVK	12.1	Tested until 1000 h (more stable than PEDOT:PSS)	76
Me-QTPA	9.07	Higher than spiro-OMeTAD (tested for 600 h. Shows hydrophobicity)	77
Me-BPZTPA	8.16	Tested for 600 h	77
FePc-Cou	9.40	Tested for 10 h	78
NiPc-Cou	10.23	Tested for 10 h	78
DEPT-SC	11.52	Tested until 250 h	79
TTPA-BDT	18.1	Show good thermal stability (value not mentioned)	80
TTPA-DTP	15.6	Show good thermal stability (value not mentioned)	80
TEOS	—	(Stable for 1200 hours)	77

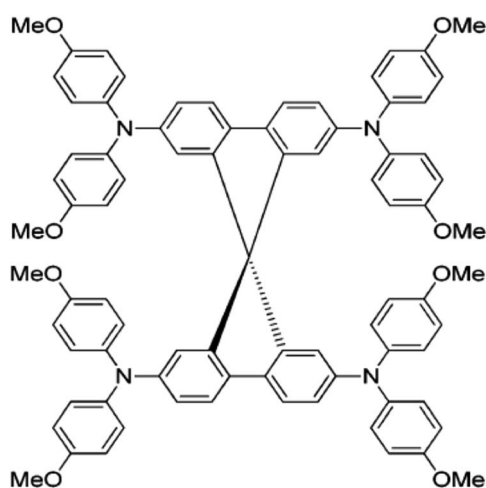


Fig. 3 Molecular structure of spiro-OMeTAD. This figure has been adapted from ref. 82 with permission from American Chemical Society.

same features as offered by spiro-OMeTAD, which are discussed below.

**Pyrene core and truxene core based HTMs.** First, alternate HTMs appeared in 2013 by Seok *et al.*<sup>82</sup> The pyrene core (as given in Fig. 4) was introduced in arylamine derivative molecules and it replaced the spiro-bifluorene core in spiro-OMeTAD. The three categories of pyrene achieved PCE of 3.3%, 12.3% and 12.4% for PY-1, PY-2 and PY-3 respectively, while under same conditions the spiro-OMeTAD exhibited PCE

of 12.7%. The lower PCE (3.3%) for PY-1 was due to insufficient hole injection. The addition of pyrene core in arylamine derivatives introduced electron-blocking capability surpassing that of spiro-OMeTAD, while keeping synthesis cost lower.<sup>82</sup> Chen *et al.*<sup>83</sup> developed a C<sub>3h</sub> truxene-core (Trux-I) using OMeTAD. Its distinct structure resulted in an excellent hole mobility, greater than the spiro-OMeTAD. Grisorio *et al.*<sup>84</sup> further modified the Trux-I and synthesized a new molecule Trux-II. In the case of p-i-n device structure both Trux-I and Trux-II exhibited better performance with PCE for Trux-I = 10.2%, Trux-II = 13.4% as compared to the reference samples using spiro-OMeTAD (with 9.5% PCE). Rakstys *et al.*<sup>85</sup> have synthesized two-dimensional triazatruxene-based derivatives series (triazatrux I-IV) using a simple synthesis procedures to produce low cost devices. Among this series triazatrux-II structure exhibited PCE of 17.7%, while spiro-OMeTAD based reference device showed PCE of 17.1%.

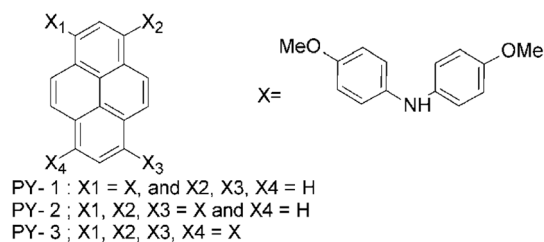


Fig. 4 Molecular structure of pyrene-based HTMs. This figure has been adapted from ref. 82 with permission from American Chemical Society.



**Phenothiazine based HTMs.** Phenothiazine is an important candidate in designing high-mobility organic semiconductors.<sup>86</sup> Structure of phenothiazine based HTMs is shown in Fig. 5. Recently, Grisorio and group developed and made two phenothiazine based (PH-I and PH-II) molecules.<sup>87</sup> When used as HTMs, PH-I realized PCE of 2.1% whereas PH-II showed PCE of 17.6% which is very near to 17.7% for spiro-OMeTAD.<sup>87</sup>

**Thiophene, bithiophene and tetrathiophene HTMs.** Liu *et al.*<sup>88</sup> have developed thiophene based HTMs (Thio-I and Thio-II) using dibromo thiophene and arylamine. PCE of 15.13% was achieved for Thio-II HTM which was 40% higher than that of Thio-I. Under same conditions spiro-OMeTAD as HTM surprisingly produced a PCE of 8.83%. Whereas, Rakstys *et al.*<sup>89</sup> prepared a bi-thiophene based derivative known as BTHIO. BTHIO based devices unveiled 19.4% PCE which was a slightly higher PCE (with improved stability) than that of reference device using spiro-OMeTAD. Also, Zimmermann *et al.*<sup>90</sup> established electron rich tetra-thiophene based HTMs (TETRATH I-IV). TETRATH-I reported 18.1% PCE along with higher thermal stability as compared to spiro-derivative. The results indicated that high performance, thermal stability and low-cost PSCs can be designed using tetrathiophene.

**Triazine based HTMs.** 12.5% and 10.9% PCEs were reported for TRIAZ-I and TRIAZ-II (as shown in Fig. 6) respectively reported by Ko and group.<sup>91</sup> Lim *et al.*<sup>92</sup> introduced two triazine-core star-shaped HTMs known as TRIAZ-III and TRIAZ-IV. They observed enhanced PCEs of 13.2 and 12.6% for TRIAZ-III and TRIAZ-IV, respectively, which are close to 13.8% achieved using spiro-OMeTAD.

**Benzotrithiophene and squaraine HTMs.** Ontoria *et al.*<sup>93</sup> have acquired three benzotrithiophene based HTMs (BZTR-I, BZTR-II and BZTR-III) using cross-coupling reactions between various benzotrithiophene and triphenylamine derivatives with 18.2% PCE. In a similar manner, Benito *et al.*<sup>94</sup> have designed tri-arm (BZTR-IV) and tetra-arm isomers (BZTR-V). The corresponding PSC devices exhibited outclass performance and achieved PCEs of 19 and 18.2% for BZTR-IV and BZTR-V, respectively with good stability under temperatures upto 430 °C. Recently, Paek *et al.*<sup>95</sup> developed squaraine-based HTMs (SQ-H, SQ-OC<sub>6</sub>H<sub>13</sub>). From these HTMs, PCEs of 14.74% for SQ-H and 14.73% for SQ-OC<sub>6</sub>H<sub>13</sub> were obtained while under same conditions the spiro-OMeTAD produced 15.33% PCE.

**Fluorene and spiro-fluorene HTMs.** Rakstys *et al.*<sup>96</sup> developed bifluorenylidene based HTM (FL-I) with a lower band gap and a HOMO level similar to spiro-OMeTAD. FL-I, 50-times less expensive than spiro-OMeTAD, showed a PCE of 17.8%, which is comparable to 18.4% produced by spiro-OMeTAD. To enhance the electrical conductivity of the device, different dopants were used in HTMs which decreased the stability while increasing cost of the device. Keeping this in view, Wang *et al.*<sup>97</sup> developed a dopant free HTM (FL-II) which comprised of poly-triarylamine unit (*N*-benzene) and spiro-OMeTAD. FL-II exhibited a PCE of 12.39% without dopants and 16.73% with dopants. While on other hand 14.84% and 5.91% values were reported using spiro-OMeTAD. Considering the device stability, Reddy and group introduced two fluorene based HTMs (FL-III and FL-IV) by Suzuki coupling reaction. Both, FL-III and FL-IV showed high hole mobility, good solubility and long-term device stability. These materials have been employed as substitute of spiro-OMeTAD in PSCs and substitute of PEDOT:PSS in organic bulk-heterojunction (BHJ). In PSC, the reported PCE was 17.25% for FL-III. While for BHJ it was 7.93%. The reference PCEs were 16.67% and 7.74% for spiro-OMeTAD and PEDOT:PSS, respectively.<sup>98</sup> Tiazkis *et al.*<sup>99</sup> have examined the characteristics of fluorene based HTMs. They observed that by replacing an aliphatic group to the *meta*- and *para*-positions of triphenylamine fragments, the charge transport, hole extraction and molecular planarity properties could be modified. In *meta*-substitution case, they observed inferior performance because of the non-favorable geometry, but in case of *para*-substitution, recorded PCE values were in the range of 9–16.8%, almost approaching the PCE of spiro-OMeTAD as a reference (17.8%).

Spiro-FL-I was designed by Bi and co-workers with excellent recorded PCE of 19.8%, comparable to that of spiro-OMeTAD (20.8%) reference sample. Also, FL-I based devices exhibited less hysteresis, outstanding reproducibility and better stability under specific (dry and dark) conditions.<sup>100</sup> Keeping in view similar design structure, 3D-spiro-fluorene-based HTMs (spiro-FL-II and spiro-FL-III) were designed by Xu *et al.*<sup>101</sup> Spiro-FL-III showed higher hole-mobility, deeper HOMO level, better solubility and improved film properties as compared to spiro-OMeTAD. The spiro-FL-III also yielded impressive PCE of 20.8% much higher than the 18.8% PCE of spiro-OMeTAD with

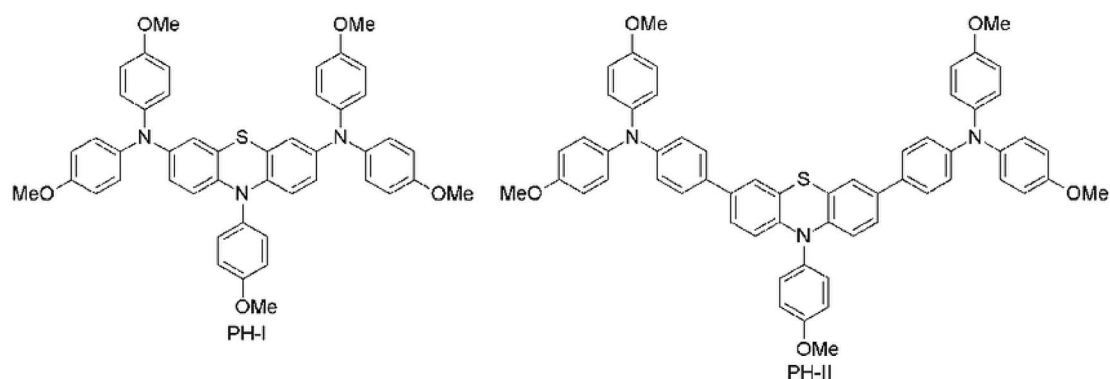


Fig. 5 Structure of phenothiazine based HTMs. This figure has been adapted from ref. 86 with permission from Springer Nature.



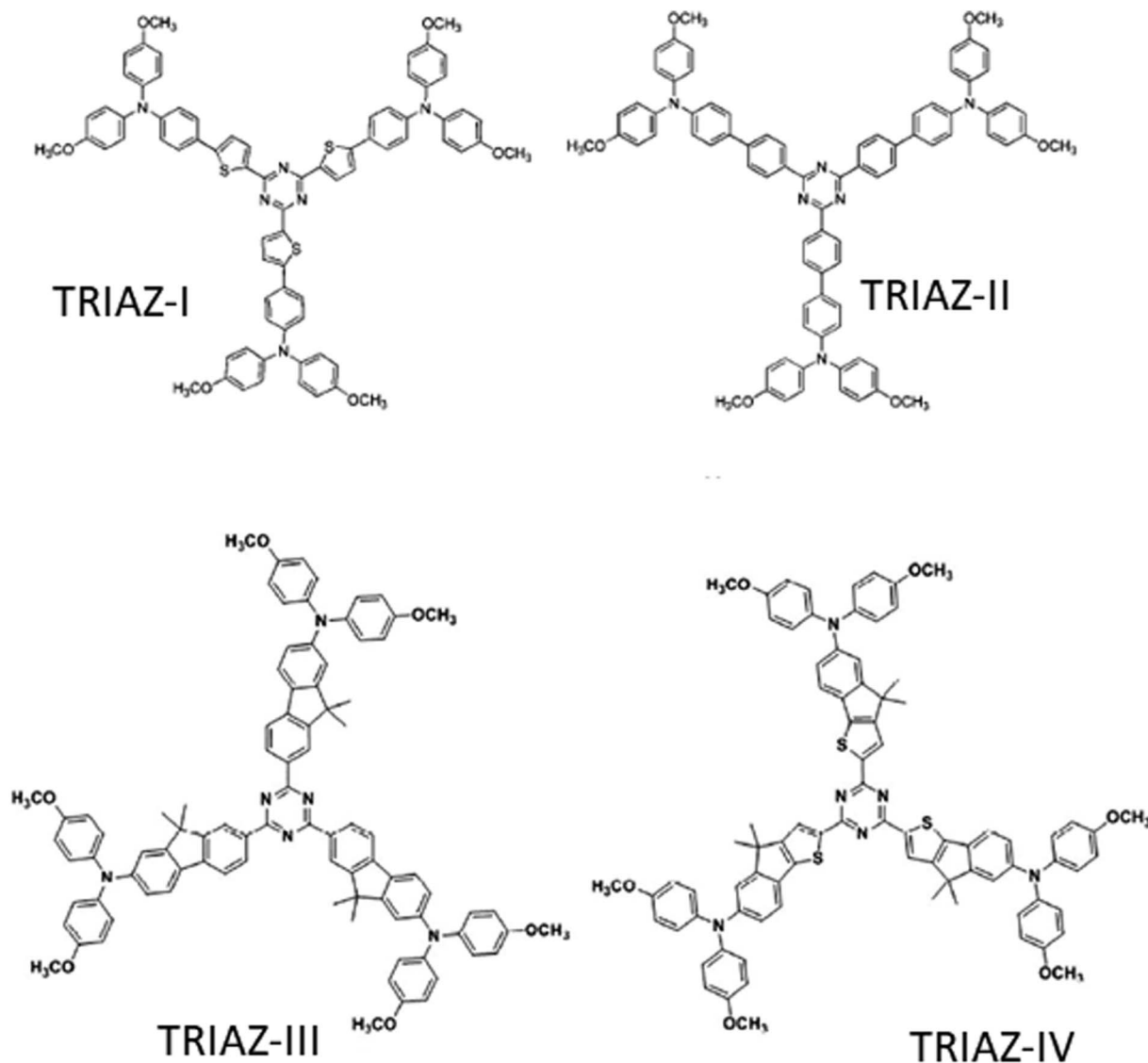


Fig. 6 Structure of triazine based HTMs. This figure has been adapted from ref. 91 with permission from Royal Society of Chemistry.

magnificent stability after six months long-term aging. However, the spiro-FL-II achieved PCE of 13.6% with same order of hole mobility as does the spiro-OMeTAD. The overall materials cost was around 1/5 as compared to spiro-OMeTAD. The reported PCE values for these HTMs were upto 20%.<sup>102</sup> Saliba *et al.*<sup>103</sup> have proposed a new class of HTMs FDT. When used as HTM in mesoscopic type configuration, the device exhibited highest PCE of 20.2% for small molecule HTMs. FDT are less expensive (~\$60 g<sup>-1</sup>) and soluble in toluene that is less hazardous than chlorobenzene, which is used to dissolve spiro-OMeTAD.

**Carbazole based HTMs.** The attractive photophysical properties like intense luminance, reversible oxidation process, low synthetic cost, flexible carbazole reactive sites and the outstanding charge transport properties make this class of compounds prominent and novel for cost effective HTMs for PSCs.<sup>67,104–114</sup> Wang *et al.*<sup>115</sup> reported a carbazole based CA-I compound made by a two-step reaction process using less expensive commercially available materials. CA-I, exhibited

good hole mobility and better conductivity than spiro-OMeTAD and showed a PCE of 12.3%.<sup>116</sup> Leijtens *et al.*<sup>106</sup> have designed two, simple lithium salt-free, carbazole based HTMs, varied by the alkyl group (CA-II and CA-III). When applied in the PSCs in oxidized form, the devices produced results comparable to spiro-OMeTAD based devices. Other examples include two arms and three arm structures, connected *via* TPA, phenylene or diphenylene core units (CA-IV, CA-V and CA-VI). Using these systems, the highest PCE of 14.79% was achieved. Wang *et al.*<sup>108</sup> developed carbazole based derivatives (CA-VII and CA-VIII) with biphenyl core.

Xu *et al.*<sup>114</sup> have demonstrated two carbazole-core based HTMs (CA-IX and CA-X). Under similar conditions, in solid state DSSCs, CA-X based device achieved PCE of 6%, higher than that of CA-IX (4.5%) and spiro-OMeTAD (5%) as a reference. Due to superior performance of CA-X as compared to CA-IX and spiro-OMeTAD in solid state DSSC, CA-X was further investigated in PSC as HTM and achieved PCE of 9.8% as compared to 10.2%



PCE obtained by spiro-OMeTAD based device as a ref. 117. Kang *et al.*<sup>109</sup> have designed a group of dendritic carbazole based star shaped HTMs (CA-XI, CA-XII and CA-XIII) and studied their performance in PSCs. Because of crystallization during the fabrication process, the trimeric structures showed good conductivity than the dimeric ones. When used as HTM, CA-XIII exhibited a PCE of 13% which is comparable to PCE of 13.76% achieved by spiro-OMeTAD based PSC. Zhang *et al.*<sup>67</sup> developed two new carbazole based materials (CA-XIV and CA-XV) utilizing commercially available di-substituted and tri-substituted phenyl derivatives. The CA-XV based PSC achieved slightly higher PCE of 13.1% as compared to 11.4% and 12.0% for CA-XIV and spiro-OMeTAD, respectively. Daskeviciene *et al.*<sup>110</sup> proposed a simple one-step synthesis for a low cost HTM (CA-XVI). When used as HTM, the PSC exhibited PCE of 17.8%, comparable to a reference device of spiro-OMeTAD. Chen *et al.*<sup>111</sup> proposed a tetra-substituted carbazole-based HTM (CA-XVII) using a three-step synthesis process and low-cost materials, which produced a PCE of 17.81%. Zhu and fellows have designed a carbazole-based molecular material using a tetraphenylene core (CA-XVIII). The device showed good thermal stability and energy levels with a PCE of 12.4%. The achieved PCE is close enough to the one obtained from doped spiro-OMeTAD device.<sup>112</sup> Zhu *et al.*<sup>113</sup> recently synthesized a chain of carbazole derivatives having variation in the 2,7 and 3,6 positions (CA-XIX, CA-XX and CA-XXII). Among these materials, the 2,7 substituted derivatives (CA-XX and CA-XIX) resulted in good stability because of highly twisted structure and PCEs of 16.74% and 14.92%, respectively. While 3,6 substituted derivative CA-XXII reported a PCE of 13.3%. Recently, Wu *et al.*<sup>118</sup> have proposed a carbazole based HTM including electron deficient benzothiadiazole (BT) core (CA-XXIII). The addition of a BT unit in biphenyl structures in CA-XXIII increased the intermolecular interactions, improved hole mobility, charge transport and thermal stability of the compound. When used as HTM, a PCE of 16.87% was reported for CA-XXIII, higher than 15.53% achieved by spiro-OMeTAD PSC.

**Hole transporting materials based on benzodithiophene and dithienopyrrole cores.** M. K. Nazeeruddin *et al.*<sup>80</sup> have observed and designed two new classes of HTMs based on benzodithiophene (BDT) and dithienopyrrole (DTP) cores. They substituted BDT and DTP central cores with four *N,N*-bis(4-methoxyphenyl) aniline units through the 2- and 3-positions of thiophene rings giving rise to the tetrakis(triphenylamine) (TTPA) derivatives. The substitution of the inner core benzene ring of BDT by a pyrrole ring in DTP allows addition of an extra heteroatom to the system, which provides a stronger electron donating characteristics. They reported that HTM based on BDT core demonstrated outclass performance with 18.1% as compared to DTP based HTM (15.6%) and spiro-OMeTAD based device (17.7%). This superior performance of TTPA-BDT based HTM was achieved due to better alignment of HOMO (−5.36 eV) with the perovskite's valence band (−5.65 eV), lower reorganization energy (0.11 eV) and higher fill factor.

**Other small molecular materials HTMs.** Zong *et al.*<sup>69</sup> have introduced two binaphthol based derivatives (NPH-I and NPH-II) which vary in the aromatic or aliphatic linkage to

binaphthol unit. The HOMO levels of both materials were well aligned with that of perovskite and PCE values reported were similar to that of spiro-OMeTAD. Li *et al.*<sup>119</sup> have designed two different HTMs by varying  $\pi$ -linker unit (biphenyl *vs.* carbazole: OMe-I and OMe-II) and obtained PCEs of 16.14% and 18.34% for OMe-I and OMe-II, respectively. Petrus *et al.*<sup>120</sup> have studied the problem of reducing HTM synthetic costs. They introduced a material with 3,4-ethylenedioxy thiophene (EDOT) as a central core (EDOT-AZO). EDOT-AZO was synthesized under ambient conditions using simple one-step Schiff base condensation chemistry of amine and aldehyde of EDOT with cost effective precursors. EDOT-AZO is the least expensive HTM reported so far in the context of PSCs (cost of EDOT-AZO is around \$10 g<sup>−1</sup>). As an HTM, EDOT-AZO reported a PCE of 11% comparable to 11.9% as obtained by spiro-OMeTAD based device.

**5.1.2. Polymer hole transport materials.** Poly(triaryl amine) (PTAA) was the first ever and the most efficient polymer based HTM, which was tested in PSCs. Seok *et al.*<sup>104</sup> used PTAA in mesoscopic structure and formed a zig-zag-like pattern; the reported PCE was 12%. Using mixed perovskites (MAPbBr<sub>3</sub> and FAPbI<sub>3</sub>) and immense optimization process, the PCE was enhanced to 20%.<sup>121,122</sup> Furthermore, PTAA is a high cost material (~\$2000 g<sup>−1</sup>).<sup>123</sup> P3HT and PEDOT:PSS are prominent conducting polymers and have been employed as HTMs.<sup>124</sup> PEDOT:PSS has been mostly employed in inverted planar PSCs and possesses features like compatible valence band with perovskite, low temperature processability and excellent film properties. The highest efficiency of 18.1% was achieved using PEDOT:PSS with hydrogen iodide (HI) as additive and perovskite.<sup>125</sup> The main constraint of PEDOT:PSS is its hygroscopic nature.

The improvement of the device stability through the introduction of the stable and efficient conducting polymer-based HTMs have been documented by Lim *et al.*<sup>126–128</sup> They reported the use of high-work function self-organized hole extraction layers (SOHELs) to attain the improved PCE.<sup>128</sup> A SOHEL accomplishes good energy level alignment with ionization potential level of CH<sub>3</sub>NH<sub>3</sub>PbI<sub>3</sub> in such a way that it increases built-in *e*-potential, *J*<sub>sc</sub>, FF and *V*<sub>oc</sub>.<sup>126,128</sup> They also compared the results of the PEDOT:PSS based PSCs with those incorporating SOHEL<sup>127</sup> and found that the offset energy at the hole extraction layer and the photoactive layer can be reduced by collective energy level alteration of the SOHEL. They also made-up a flexible PSC on PET/ITO substrate using SOHEL and reported the PCE as high as 8.0%.<sup>128</sup>

Dubey *et al.*<sup>129</sup> reported a diketopyrrolopyrrole based polymer known as PDPP3T and achieved a PCE of 12.32% comparable to 12.34% reported for spiro-OMeTAD based PSC. An additional interesting attribute, the PDPP3T based PSC produced slower device degradation having a decrease in PCE to 60.6% of its initial value in 172 h. On the other hand, spiro-OMeTAD based device decreased the PCE to 83% of its initial level in the same time. Stringer *et al.*<sup>130</sup> have reported a carbazole based co-polymer, PCDTBT, a familiar donor material in organic BHJ devices. The PCDTBT device after being doped with LiTFSI and TBP achieved a PCE of 15.9% almost equal to that of spiro-OMeTAD device. Yu *et al.*<sup>131</sup> investigated a co-polymer



based on PCPDTBT. The highest ever reported PCE of 15.1% was achieved for PCPDTBT based polymers, when PCPDTBT was doped with 2,3,5,6-tetrafluoro-7,7,8,8-tetracyanoquinodimethane (F4TCNQ). Zhou *et al.*<sup>132</sup> have designed a hyper-branched carbazole based polymer (HB-CZ) using one-step Suzuki coupling method. When employed as HTM, the device showed a PCE of 14.07%, higher than the PCE of 9.05% and 6.60% reported for P3HT and PCz based devices, respectively. Liu *et al.*<sup>133</sup> have proposed a highly  $\pi$ -extended copolymer PDVT-10 as HTM with an excellent hole mobility of  $8.2 \text{ cm}^2 \text{ V}^{-1} \text{ s}^{-1}$  and achieved a PCE of 13.4% without doping that is considered the highest reported PCEs for dopant-free polymer HTMs.

Liu and fellows have proposed a carbazole based non-conjugated polymer (PVCz-OMeDAD), having a non-conjugated polyvinyl sequence and a hole transporting OMeDAD unit.<sup>133</sup> The OMeDAD moiety increased hole transporting potential of the material. The PCE of 16.09% was observed, which is, much better than that of 9.62% obtained by spiro-OMeTAD based device used as a reference. Gaml *et al.*<sup>134</sup> have implemented benzodithiophene based polymer PBDTT-FTTE, as hole transporting material in PSCs. After doping, 3% of diiodooctane with PBDTT-FTTE, the device exhibited same performance as traditional spiro-OMeTAD based devices in an inert atmosphere with increased FF and  $V_{oc}$ . Diiodooctane doped PBDTT-FTTE device achieved a PCE of 11.6%, whereas on the other hand the un-doped PBDTT-FTTE based cells exhibited a PCE of 10.3%.

**5.1.3. Dopant free hole transport materials.** Hole transportation materials (HTMs) play a key role in the performance of highly efficient PSCs. As mentioned earlier, spiro-OMeTAD has been the most widely used HTM. But, spiro-OMeTAD suffers an insufficient hole transportation and low conductivity in its pristine form. Therefore, additives/dopants like lithium bis(trifluoromethanesulfonyl)imide (Li-TFSI),<sup>24,25,26</sup> 4-*tert*-butylpyridine (TBP),<sup>26</sup> and tris(2-(1*H*-pyrazol-1-yl)-4-*tert*-butylpyridine)cobalt(III) tri[hexafluorophosphate] (FK209)<sup>26</sup> are used to generate free carriers and to enhance conductivity. However, these dopants affect the device performance and stability.

For this purpose, the development of cost effective dopant free HTMs with improved moisture resistance and carrier transport properties is required for stable and efficient PSCs. Huang *et al.*<sup>83</sup> demonstrated PCE of 18.6% using a dopant free HTM Trux-OMeTAD, comprising  $C_{3H}$ , Truxene-core with arylamine terminals and hexyl side chains. M. K. Nazeeruddin *et al.*<sup>62</sup> introduced rigid quinolizino acridine (FA-CN) and a flexible triphenylamine (TPA-CN) as dopant free HTMs and exhibited PCEs of 18.9% and 17.5% for FA-CN and TPA-CN, respectively, under full sun illumination. M. K. Nazeeruddin and fellows successfully developed three symmetrical dopant-free HTMs (KR321, KR353 and KR355) using D- $\pi$ -A type architecture. Among these three HTMs, the optimized structure of KR321 based device showed improved performance with a PCE of  $\sim 19\%$  along with improved stability.<sup>135</sup> Heo *et al.*<sup>136</sup> investigated DFBT (DTS-FBTTh<sub>2</sub>)<sub>2</sub> dopant free HTM using D'-A-D-A-D-A-D' (D, D': electron donors, A: electron acceptor)

conjugated structure and achieved 17.3% PCE. Lee and group members demonstrated 18.3% PCE using green solvent processable polymer HTM composed of benzothiadiazole (BT) and benzo[1,2-*b*:4,5-*b'*]dithiophene (BDT) (asy-PBTBDT).<sup>137</sup>

## 5.2. Inorganic hole transport materials

From the past several years, inorganic materials have been studied and implemented as hole transporting materials due to their unique properties such as appropriate energy levels, good hole mobility, high chemical stability and low fabrication cost. However, problem associated with this type of HTMs is the device stability introduced by a solvent, which can partially dissolve the perovskite. Nickel oxide (NiO) is the most promising wide band gap p-type material that was successfully used as HTMs in DSSC and OPV devices. It has been implemented in various device structures, like mesoporous carbon electrode-based PSCs, inverted mesoscopic PSCs and inverted planar based PSCs. Sarkar *et al.*<sup>138</sup> achieved a PCE of 7.26% by depositing NiO layer on an inverted planar type configuration using electrodeposition. Chen *et al.*<sup>139</sup> enhanced the performance of NiO layer and achieved PCE of 11.6% under one-sun-illumination by varying the thickness and using oxygen doping. Recently, low temperature solution processed NiOx was implemented as HTM in n-i-p and p-i-n PSCs structures. The considerable accomplishment of this work was to present direct deposition of pre-synthesized NiOx on the top of perovskite layer (in n-i-p assemblies) without rotting the perovskite film. The considerable PCE of 15.9% was obtained with negligible hysteresis.<sup>140</sup> Duc *et al.*<sup>141</sup> used NiO as HTM in perovskite based inverted planar configuration and reported a PCE over 16%.

Copper (Cu) has also been successfully investigated to design cost effective and solution processable Cu based inorganic HTMs. Kamat *et al.*<sup>142</sup> studied copper iodide (CuI) based device and reported overall PCE of 6%. The low efficiency was due to low  $V_{oc}$ . Other interesting examples of this class of materials include cupric cuprous oxide (Cu<sub>2</sub>O) and copper thiocyanate (CuSCN). Cu<sub>2</sub>O is a narrow band gap, low cost, environmental friendly material with good hole mobility. For such type of material, the reported PCE was 8.93% with good stability over 30 days in the open air.<sup>143,144</sup> In 2014, Gratzel *et al.*<sup>145</sup> performed considerable work on CuSCN as HTM and achieved 12.4% PCE. CuSCN HTM demonstrated performance owing to effective charge extraction and charge transportation from perovskite layer to top electrode. Moreover, a considerable PCE over 16% was reported by Nazeeruddin *et al.*<sup>146</sup> for PSCs using mixed perovskite (FAPbI<sub>3</sub> and MAPbBr<sub>3</sub>) in addition to CuSCN as p-type hole transport material.

## 5.3. Hybrid hole transport materials

Y. Kwon used poly[2,5-bis(2-decyldodecyl)pyrrolo[3,4-*c*]pyrrole-1,4(2*H*,5*H*)-dione-(*E*)-1,2-di(2,20-bithiophen-5-yl)ethene] (PDPPDBTE) as a p-type HTM on a hybrid organic-inorganic perovskite solar cell.<sup>147</sup> The hydrophobicity of the polymer prevented moisture permeation on the porous perovskite heterojunction. Z. Fei *et al.*<sup>63</sup> used thiophene based HTMs (Z25, Z26) to achieve 20.1% efficiency which is similar to spiro-OMeTAD. The



HTM Z26 showed more stability than spiro-OMeTAD and Z25. The presence of a double bond in the structure of Z26 made the HTM more stable. Thiophenes are semi-conductors in nature. Higher hole mobility of thiophene make them an attractive HTM material. Their interaction with iodine promote photo-generated hole transport. X. Liang *et al.*<sup>148</sup> argues that HTMs with high thermal stability and high hole mobility are rare. Phenothiazine based HTM, SFX-PT1 and SFX-PT2, were developed and found to be more stable than spiro-PT and spiro-OMeTAD. Moreover, SFX-PT1, SFX-PT2 and perovskite have comparable energy levels which make them compatible. However, SFX-PT1 and SFX-PT2 showed low solubility, which might be a problem for large scale application.

According to W. Yei *et al.*<sup>71</sup> HTM made of silver doped NiOx(Ag:NiOx) showed better performance for an inverted planar heterojunction perovskite solar cell. In Ag:NiOx, Ag occupies the substitutional Ni sites and behaves as an acceptor in NiO lattice. Doping with silver increases hole mobility, conductivity and stability of NiOx film. The stability of this novel HTM compared to organic HTMs is drastically higher. Xie *et al.*<sup>149</sup> reported a high efficiency HTM  $\text{Li}_{0.05}\text{Mg}_{0.15}\text{Ni}_{0.8}\text{O}$  as an alternative to original NiOx, which is attributed to enhanced hole conductivity and charge extraction. According to K. Im, Ti doped  $\text{MoO}_2$  has high thermal stability due to strong Mo–O bond.<sup>74</sup> Moreover, the compound is highly stable in humidity as well. Another advantage of this HTM is its scalability. Although the compound is stable in humidity,  $\text{MoO}_2$  has the tendency to oxidize itself to  $\text{MoO}_3$  in the air. However, doping with titanium solves this problem to some extent.

H. Li *et al.*<sup>150</sup> reports similar stability of 3,4-ethylenedioxythiophene and 9'-spirobifluorene (spiro-OMeTAD) which is a widely used HTM. Habisreutinger *et al.*<sup>40</sup> proposed polymer-functionalized single walled carbon nano-tube (SWNT) embedded in an insulating polymer matrix as HTM. Strong retardation of thermal degradation was observed in the cell as compared to organic HTMs. Moreover, the proposed HTM was found to be water resistant. Perovskite and organic HTMs degrade fast under heat. If poly(methyl methacrylate) (PMMA) is used for coating perovskite, its thermal stability increases. But, the coating acts as an insulator as it lacks  $\pi$ -conjugation. However, combining this insulator with highly conductive single walled carbon nano-tube, the properties of conventional HTMs can be achieved along with durability. Carbon nanotubes (CNTs) are generally insoluble, however when wrapped with a monolayer of P3HT, they form supramolecular nano-hybrids (P3HT/SWNT) that are dispersible in common solvents and can be deposited by spin-coating.

## 6. Limitations of HTMs

Organic HTMs have several drawbacks including unspecified molecular-weight, low purity and batch-to-batch variation.<sup>105,151,152</sup> The amorphous nature of small molecule-based hole transport materials imparts poor hole mobility. Among organic HTMs, polymers are well known for their good hole mobility, strong chemical interaction with perovskite and highest efficiency. These material have high molecular weight

which doesn't allow easy penetration hooked on the openings of  $\text{TiO}_2$  scaffold.<sup>152</sup> Similarly, PEDOT:PSS with successful outcomes has a well known drawback of hygroscopic nature, which restricts the chemical-stability of PEDOT:PSS based devices in an ambient environment.<sup>152</sup> In case of hydrophilic materials, all deposition processes need to be carried out in gas filled glove box and the measurements are performed with relative humidity (%RH) < 1 and under controlled atmospheric conditions.<sup>12</sup> To solve this problem, several types of dopants are used. Unfortunately, these dopants decrease device stability and ultimately degrade the PSCs.<sup>152</sup> For the process of hole extraction, adequate hole transportation and conductivity are required. In regular n-i-p structures, a thick HTM layer is normally deposited to acquire a pinhole free surface on the perovskite. But, a thick HTM layer produces high series resistance that leads to lower FF and PV performance. To overcome this issue, p-type doping is commonly used to enhance hole mobility and conductivity of HTMs. However, an introduction of additives can affect the device stability, especially for hydrophilic components that can degrade the perovskite crystals.<sup>153</sup> In case of inorganic hole transport materials, the most common problem is their solvents which can partially dissolve the perovskite and consequently affect device performance and stability.<sup>152</sup> Whereas the transition metal oxides as HTMs hold a very impoverished film morphology which results in extremely low quality films.<sup>152</sup>

## 7. Research agenda for future studies

The hole transport materials have significant effect on open circuit voltage ( $V_{oc}$ ) of the cells as they decrease recombination resistance and increase series resistance. Apart from the properties and improved efficiencies several challenges need to be addressed before the successful development and commercialization of the PSCs. These challenges include hysteresis, reproducibility of efficient devices, toxicity as well as thermal and chemical stability. These factors directly or indirectly affect the stability of the PSCs. The stability of cells is a main hurdle in the commercialization of PSCs. Various approaches have been adopted with an aim to enhance the stability of PSCs, but they have failed to improve long-term performance of PSCs and the issue is still under debate. Of course, cost must also be kept in mind while considering the stability issues. If we take a close look at the energy levels/work function (given in Table 1) of the possible HTMs used in PSCs, it can be observed that spiro-OMeTad has least stability however it results in greater efficiency. P3HT with an  $E_g$  of 2 eV showed an efficiency of 20% and remained stable for 800 h. Similarly, the work function of the engineered PEDOT:PSS demonstrated better stability than the pristine PEDOT:PSS. Hence by gathering the facts regarding relation between performance and energy/level/work function, it can be inferred that LUMO/work function beyond 5 eV leads to better performance of the device.

Thermal and chemical stabilities are also very important issues which also need to be addressed properly, thermal treatment is required in the process of formation of perovskite crystals. Both annealing and storage temperatures are main



factors due to which degradation in PSCs occurs. Thermal instability due to HTM can be reduced using HTM free perovskites solar cells. Excellent thermal stability has been reported with HTM free PSCs. For example, L. Etgar *et al.*<sup>154</sup> were the first to report HTM-free MPSC with a 5.5% PCE. Later in 2014, they reported enhanced efficiency of HTM-free MPSC to 10.85%.<sup>155</sup> Han and co-workers reported fully printable HTM-free MPSC based on triple mesoscopic layers of low-cost carbon counter electrode, mesoporous  $\text{ZrO}_2$  and  $\text{TiO}_2$ .<sup>156</sup> The device exhibited good stability and a PCE of 6.64%. Li *et al.*<sup>31</sup> performed some stability tests to check performance of the printable HTM-free MPSC using  $(5\text{-AVA})_x(\text{MA})_{1-x}\text{PbI}_3$ . The devices remained stable when exposed outdoors in Jeddah, Saudia Arabia for a period of consecutive seven days. Furthermore, stable PSC was also reported when the encapsulated device was thermally tested at 80–85 °C for 90 days. Moisture penetration in hole transporting layer can be restricted by crosslinking the layer. Xu *et al.*<sup>157</sup> reported thermally cross-linked arylamine derivative ( $N4,N4'$ -di(naphthalen-1-yl)- $N4,N4'$ -bis(4-vinylphenyl)biphenyl-4,4'-diamine) (VNBp). (VNBp).

Electron blocking layer (ETL) can also be used before the HTM layer and an HTM layer is used before ETL to restrict the overflow of electron and hole at either side as well as to reduce the moisture penetration. Xu *et al.*<sup>157</sup> used double layers of VNBp- $\text{MoO}_3$  and achieved better stability under harsh conditions. The hysteresis is also an important issue which might be closely related with long-term stability of the devices.<sup>158,159</sup> There are few possible reasons for the hysteresis in organic perovskite solar cells which include charge trapping,<sup>158</sup> ion migration,<sup>18,21,160</sup> ferro electricity<sup>161–163</sup> and capacitive effects.<sup>164,165</sup> By properly controlling all these factors, hysteresis effects can be reduced.

The cost is another crucial factor that needs to be addressed beside the stability to introduce PSC technology to the commercial market for instance, the cost of purified spiro-OMeTAD is  $\sim \$500\text{--}1000 \text{ g}^{-1}$ .<sup>81,166</sup> The factors which affect the cost of HTMs include complex and costly systems required for purification process. Search for cost effective HTMs started since the first PSC was introduced. Zhang *et al.*<sup>167</sup> reported a cost-effective dopant free P3HT as a replacement to spiro-MeOTAD. Later, Xiao and co-workers demonstrated a new class of solar cell with polyaniline (PANI) as a sensitizer and as a p-type hole transporting material.<sup>168</sup> In their work, they achieved a PCE of 7.34% along with long-term stability. Similarly, few researchers have employed inorganic hole transport materials. Christians *et al.*<sup>142</sup> reported CuI as a hole transport material. Using cost effective, stable and solution-processable inorganic material, they showed a remarkable efficiency of 6.0% close to that of 7.9% (obtained for spiro-OMeTAD based device). However, there must be balance between the cost and efficiency.

To achieve best performance of PSCs, HTMs must fulfill following general requirements.

(1) The highest occupied molecular orbital (HOMO) energy level should be compatible with the valence band energy (VBE) of the perovskite.

(2) For efficient hole transportation from perovskite absorber, HTMs must have sufficient charge carrier mobility (which ideally should be greater than  $10^{-3} \text{ cm}^2 \text{ V}^{-1} \text{ s}^{-1}$ )

(3) HTMs must have air, moisture, photochemical and thermal stability.

(4) Ideally, HTMs should be solvable in various organic solvents and have exceptional film formation capability for device fabrication and processing.

(5) HTMs should be low cost and have environmental friendly behavior.

In summary, up to now, a selection of organic, inorganic and hybrid HTMs have been reported in both standard and inverted PSC configurations. To enhance the PCE and stability of the PSCs, the following facts related to HTM must be considered. For the better PCEs, a good energy level alignment and interface compatibility should be taken into account, primarily. From the HTM-film quality optimization perspective, it is of utmost priority that a high-quality consistent HTM film must be prepared with less defects and desirable conductivity. Such HTMs can be achieved by optimizing or developing suitable deposition techniques. As far as the stability is concerned, additional emphasis should be put on interface engineering, compatibility and charge transfer kinetics. Furthermore, detailed understanding of interface charge transfers and recombination is necessary for developing new HTMs for stable and efficient PSCs.

## 8. Conclusion

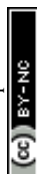
During the past few years, intensive research interest from photovoltaic research community has been paid to PSCs. Perovskites are particularly considered for photovoltaic applications because they can be obtained from cheap earth-abundant materials, processed in solution and show high device performance which is comparable with already implemented commercial technologies. Various techniques have been adopted to boost the power conversion efficiency (PCE) of PSCs. However, one key issue to approaching the market with any strategy is the long-term operational stability of PSC devices. In this review, the stability issues in PSCs and the role of HTMs on the stability and their proposed solutions have been discussed. It can be summarized that the integration of several types of approaches including interface engineering, composition engineering and development of hybrid HTMs and perovskite-inorganic HTM composites besides organic HTMs, might be important strategies for achieving high efficiency and better stability of PSCs.

## Conflicts of interest

There are no conflicts to declare.

## Acknowledgements

This work is supported by Qatar University Internal Grant No. QUCG-CAM-2018/19-1. The findings achieved herein are solely the responsibility of the authors.



## References

- 1 M. A. Green, A. Ho-Baillie and H. J. Snaith, *Nat. Photonics*, 2014, **8**, DOI: 10.1038/nphoton.2014.2134.
- 2 A. Kojima, K. Teshima, T. Miyasaka and Y. Shirai, *214th ECS Meeting*, ECS, 2014.
- 3 A. Kojima, K. Teshima, T. Miyasaka and Y. Shirai, *210th ECS Meeting*, ECS, 2006.
- 4 A. Kojima, K. Teshima, Y. Shirai and T. Miyasaka, *J. Am. Chem. Soc.*, 2009, **131**, 6050–6051.
- 5 J.-H. Im, C.-R. Lee, J.-W. Lee, S.-W. Park and N.-G. Park, *Nanoscale*, 2011, **3**, 4088–4093.
- 6 A. Yusoff, R. bin Mohd, J. Kim, J. Jang and M. K. Nazeeruddin, *ChemSusChem*, 2016, **9**, 1736–1742.
- 7 H.-S. Kim, C.-R. Lee, J.-H. Im, K.-B. Lee, T. Moehl, A. Marchioro, S.-J. Moon, R. Humphry-Baker, J.-H. Yum and J. E. Moser, *Sci. Rep.*, 2012, **2**, 591.
- 8 M. M. Lee, J. Teuscher, T. Miyasaka, T. N. Murakami and H. J. Snaith, *Science*, 2012, **04**, 1228604.
- 9 J. H. Heo, S. H. Im, J. H. Noh, T. N. Mandal, C.-S. Lim, J. A. Chang, Y. H. Lee, H.-j. Kim, A. Sarkar and M. K. Nazeeruddin, *Nat. Photonics*, 2013, **7**, 486.
- 10 J. H. Noh, S. H. Im, J. H. Heo, T. N. Mandal and S. I. Seok, *Nano Lett.*, 2013, **13**, 1764–1769.
- 11 A. J. Huckaba, S. Gharibzadeh, M. Ralaifarisoa, C. Roldán-Carmona, N. Mohammadian, G. Grancini, Y. Lee, P. Amsalem, E. J. Plichta and N. Koch, *Small Methods*, 2017, **1**, 1700250.
- 12 J. Burschka, N. Pellet, S.-J. Moon, R. Humphry-Baker, P. Gao, M. K. Nazeeruddin and M. Grätzel, *Nature*, 2013, **499**, 316.
- 13 W. Tress, N. Marinova, T. Moehl, S. M. Zakeeruddin, M. K. Nazeeruddin and M. Grätzel, *Energy Environ. Sci.*, 2015, **8**, 995–1004.
- 14 A. Yusoff, R. bin Mohd, J. Kim, J. Jang and M. K. Nazeeruddin, *ChemSusChem*, 2016, **9**, 1736–1742.
- 15 N. J. Jeon, J. H. Noh, Y. C. Kim, W. S. Yang, S. Ryu and S. I. Seok, *Nat. Mater.*, 2014, **13**, 897.
- 16 C. K. Teak, T. Olga, R. C. Cristina, I. Mine, G. Paul, G. Giulia, G. Peng, M. Tomasz, P. Wojciech, R. P. Y., T. Tomás and N. M. Khaja, *Adv. Energy Mater.*, 2017, **7**, 1601733.
- 17 N. J. Jeon, J. H. Noh, W. S. Yang, Y. C. Kim, S. Ryu, J. Seo and S. I. Seok, *Nature*, 2015, **517**, 476.
- 18 P. Sanghyun, Q. Peng, L. Yonghui, C. K. Taek, G. Peng, G. Giulia, O. Emad, G. Paul, R. Kasparas, S. A. Al-Muhtaseb, L. Christian, K. Jaeyung and N. M. Khaja, *Adv. Mater.*, 2017, **29**, 1606555.
- 19 A. D. Jodlowski, C. Roldán-Carmona, G. Grancini, M. Salado, M. Ralaifarisoa, S. Ahmad, N. Koch, L. Camacho, G. De Miguel and M. K. Nazeeruddin, *Nat. Energy*, 2017, **2**, 972.
- 20 Y. Zhang, G. Grancini, Y. Feng, A. M. Asiri and M. K. Nazeeruddin, *ACS Energy Lett.*, 2017, **2**, 802–806.
- 21 M. Saliba, T. Matsui, J.-Y. Seo, K. Domanski, J.-P. Correa-Baena, M. K. Nazeeruddin, S. M. Zakeeruddin, W. Tress, A. Abate and A. Hagfeldt, *Energy Environ. Sci.*, 2016, **9**, 1989–1997.
- 22 D. B. Michele, D. E. Giorgio, G. Marina, D. I. Valerio, N. Stefanie, K. A. R. Srimath, G. Giulia, B. Maddalena, P. Mirko, B. J. M., C. Mario and P. Annamaria, *Adv. Energy Mater.*, 2016, **6**, 1501453.
- 23 M. Qian, M. Li, X.-B. Shi, H. Ma, Z.-K. Wang and L.-S. Liao, *J. Mater. Chem. A*, 2015, **3**, 13533–13539.
- 24 M. Qian, M. Li, X.-B. Shi, H. Ma, Z.-K. Wang and L.-S. Liao, *J. Mater. Chem. A*, 2015, **3**, 13533–13539.
- 25 Z.-K. Wang, M. Li, D.-X. Yuan, X.-B. Shi, H. Ma and L.-S. Liao, *ACS Appl. Mater. Interfaces*, 2015, **7**, 9645–9651.
- 26 Y.-H. Lou and Z.-K. Wang, *Nanoscale*, 2017, **9**, 13506–13514.
- 27 W. Jin-Miao, W. Zhao-Kui, L. Meng, Z. Cong-Cong, J. Lu-Lu, H. Ke-Hao, Y. Qing-Qing and L. Liang-Sheng, *Adv. Energy Mater.*, 2018, **8**, 1701688.
- 28 L. Meng, W. Zhao-Kui, Y. Ying-Guo, H. Yun, F. Shang-Lei, W. Jin-Miao, G. Xing-Yu and L. Liang-Sheng, *Adv. Energy Mater.*, 2016, **6**, 1601156.
- 29 Z.-K. Wang, X. Gong, M. Li, Y. Hu, J.-M. Wang, H. Ma and L.-S. Liao, *ACS Nano*, 2016, **10**, 5479–5489.
- 30 G. Niu, X. Guo and L. Wang, *J. Mater. Chem. A*, 2015, **3**, 8970–8980.
- 31 R. Yaoguang, L. Linfeng, M. Anyi, L. Xiong and H. Hongwei, *Adv. Energy Mater.*, 2015, **5**, 1501066.
- 32 R. Yaoguang, L. Linfeng, M. Anyi, L. Xiong and H. Hongwei, *Adv. Energy Mater.*, 2015, **5**, 1501066.
- 33 L. Zheng, Y.-H. Chung, Y. Ma, L. Zhang, L. Xiao, Z. Chen, S. Wang, B. Qu and Q. Gong, *Chem. Commun.*, 2014, **50**, 11196–11199.
- 34 N. Aristidou, I. Sanchez-Molina, T. Chotchuangchutchaval, M. Brown, L. Martinez, T. Rath and S. A. Haque, *Angew. Chem., Int. Ed.*, 2015, **54**, 8208–8212.
- 35 T. Leijtens, G. E. Eperon, S. Pathak, A. Abate, M. M. Lee and H. J. Snaith, *Nat. Commun.*, 2013, **4**, 2885.
- 36 S. Ito, S. Tanaka, K. Manabe and H. Nishino, *J. Phys. Chem. C*, 2014, **118**, 16995–17000.
- 37 N. Chander, A. Khan, P. Chandrasekhar, E. Thouti, S. K. Swami, V. Dutta and V. K. Komarala, *Appl. Phys. Lett.*, 2014, **105**, 033904.
- 38 A. Dualeh, P. Gao, S. I. Seok, M. K. Nazeeruddin and M. Grätzel, *Chem. Mater.*, 2014, **26**, 6160–6164.
- 39 A. Pisoni, J. Jacimovic, O. S. Barisic, M. Spina, R. Gaál, L. Forró and E. Horváth, *J. Phys. Chem. Lett.*, 2014, **5**, 2488–2492.
- 40 S. N. Habisreutinger, T. Leijtens, G. E. Eperon, S. D. Stranks, R. J. Nicholas and H. J. Snaith, *Nano Lett.*, 2014, **14**, 5561–5568.
- 41 C. Bert, D. Jeroen, G. Nicolas, B. Aslihan, D. H. Jan, D. O. Lien, E. Anitha, V. Jo, M. Jean, M. Edoardo, A. F. De and B. Hans-Gerd, *Adv. Energy Mater.*, 2015, **5**, 1500477.
- 42 R. K. Misra, S. Aharon, B. Li, D. Mogilyansky, I. Visoly-Fisher, L. Etgar and E. A. Katz, *J. Phys. Chem. Lett.*, 2015, **6**, 326–330.
- 43 H. S. Kim, J. Y. Seo and N. G. Park, *ChemSusChem*, 2016, **9**, 2528–2540.



- 44 B. Philippe, B.-W. Park, R. Lindblad, J. Oscarsson, S. Ahmadi, E. M. Johansson and H. k. Rensmo, *Chem. Mater.*, 2015, **27**, 1720–1731.
- 45 B. Li, Y. Li, C. Zheng, D. Gao and W. Huang, *RSC Adv.*, 2016, **6**, 38079–38091.
- 46 J. W. Lee, D. J. Seol, A. N. Cho and N. G. Park, *Adv. Mater.*, 2014, **26**, 4991–4998.
- 47 W. Feng, Y. Hui, X. Haihua and Z. Ni, *Adv. Funct. Mater.*, 2015, **25**, 1120–1126.
- 48 Y. Fu, H. Zhu, A. W. Schrader, D. Liang, Q. Ding, P. Joshi, L. Hwang, X. Zhu and S. Jin, *Nano Lett.*, 2016, **16**, 1000–1008.
- 49 Z. Wang, Z. Shi, T. Li, Y. Chen and W. Huang, *Angew. Chem., Int. Ed.*, 2017, **56**, 1190–1212.
- 50 J. Liu, Y. Wu, C. Qin, X. Yang, T. Yasuda, A. Islam, K. Zhang, W. Peng, W. Chen and L. Han, *Energy Environ. Sci.*, 2014, **7**, 2963–2967.
- 51 J. Shi, J. Dong, S. Lv, Y. Xu, L. Zhu, J. Xiao, X. Xu, H. Wu, D. Li and Y. Luo, *Appl. Phys. Lett.*, 2014, **104**, 063901.
- 52 J. Yang, B. D. Siempelkamp, E. Mosconi, F. De Angelis and T. L. Kelly, *Chem. Mater.*, 2015, **27**, 4229–4236.
- 53 Y. Chen, B. Li, W. Huang, D. Gao and Z. Liang, *Chem. Commun.*, 2015, **51**, 11997–11999.
- 54 S. N. Habisreutinger, D. P. McMeekin, H. J. Snaith and R. J. Nicholas, *APL Mater.*, 2016, **4**, 091503.
- 55 L. Jin-Wook, K. Deok-Hwan, K. Hui-Seon, S. Seung-Woo, C. S. Min and P. Nam-Gyu, *Adv. Energy Mater.*, 2015, **5**, 1501310.
- 56 J. H. Noh, S. H. Im, J. H. Heo, T. N. Mandal and S. I. Seok, *Nano Lett.*, 2013, **13**, 1764–1769.
- 57 Improving the Long-Term Stability of Perovskite Solar Cells with a Porous Al<sub>2</sub>O<sub>3</sub> Buffer Layer.
- 58 W. Li, W. Zhang, S. Van Reenen, R. J. Sutton, J. Fan, A. A. Haghighirad, M. B. Johnston, L. Wang and H. J. Snaith, *Energy Environ. Sci.*, 2016, **9**, 490–498.
- 59 R. Bart, K. C. Gödel, P. Sandeep, S. Aditya, B. J. P. Correa, B. D. Wilts, H. J. Snaith, W. Ulrich, G. Michael, S. Ullrich and A. Antonio, *Adv. Energy Mater.*, 2016, **6**, 1501868.
- 60 I. Hwang and K. Yong, *ACS Appl. Mater. Interfaces*, 2016, **8**, 4226–4232.
- 61 C. Jiangzhao, S. Ja-Young and P. Nam-Gyu, *Adv. Energy Mater.*, 2018, **8**, 1702714.
- 62 P. Sanghyun, Q. Peng, L. Yonghui, C. K. Taek, G. Peng, G. Giulia, O. Emad, G. Paul, R. Kasparas, S. A. Al-Muhtaseb, L. Christian, K. Jaejung and N. M. Khaja, *Adv. Mater.*, 2017, **29**, 1606555.
- 63 F. Zhang, Z. Wang, H. Zhu, N. Pellet, J. Luo, C. Yi, X. Liu, H. Liu, S. Wang and X. Li, *Nano Energy*, 2017, **41**, 469–475.
- 64 H. Zheng, G. Liu, C. Zhang, L. Zhu, A. Alsaedi, T. Hayat, X. Pan and S. Dai, *Sol. Energy*, 2018, **159**, 914–919.
- 65 R. Azmi, S. Y. Nam, S. Sinaga, Z. A. Akbar, C.-L. Lee, S. C. Yoon, I. H. Jung and S.-Y. Jang, *Nano Energy*, 2018, **44**, 191–198.
- 66 Q. Chen, *et al.*, *Dyes Pigm.*, 2017, **147**(suppl. C), 113–119.
- 67 M.-D. Zhang, B.-H. Zheng, Q.-F. Zhuang, C.-Y. Huang, H. Cao, M.-D. Chen and B. Wang, *Dyes Pigm.*, 2017, **146**, 589–595.
- 68 E. Nouri, *et al.*, *Electrochim. Acta*, 2016, **222**(suppl. C), 875–880.
- 69 X. Zong, W. Qiao, Y. Chen, Z. Sun, M. Liang and S. Xue, *Tetrahedron*, 2017, **73**, 3398–3405.
- 70 J.-J. Guo, *et al.*, *Sol. Energy*, 2017, **155**(suppl. C), 121–129.
- 71 Y. Wei, *et al.*, *Appl. Surf. Sci.*, 2018, **427**(part B), 782–790.
- 72 S. K. Muduli, *et al.*, *J. Power Sources*, 2017, **371**(suppl. C), 156–161.
- 73 J. Niu, *et al.*, *Org. Electron.*, 2017, **48**(suppl. C), 165–171.
- 74 K. Im, *et al.*, *Chem. Eng. J.*, 2017, **330**(suppl. C), 698–705.
- 75 L. Calió, *et al.*, *Sol. Energy Mater. Sol. Cells*, 2017, **163**(suppl. C), 237–241.
- 76 L. Yang, Y. Yan, F. Cai, J. Li and T. Wang, *Sol. Energy Mater. Sol. Cells*, 2017, **163**, 210–217.
- 77 M. Sun, *et al.*, *Appl. Surf. Sci.*, 2017, **416**(suppl. C), 124–132.
- 78 P. Qi, *et al.*, *Synth. Met.*, 2017, **226**(suppl. C), 1–6.
- 79 G. Gong, N. Zhao, J. Li, F. Li, J. Chen, Y. Shen, M. Wang and G. Tu, *Org. Electron.*, 2016, **35**, 171–175.
- 80 R. Sandoval-Torrientes, I. Zimmermann, J. Calbo, J. Aragón, J. Santos, E. Ortí, N. Martín and M. Nazeeruddin, *J. Mater. Chem. A*, 2018, **6**, 5944–5951.
- 81 P. Vivo, J. K. Salunke and A. Priimagi, *Materials*, 2017, **10**, 1087.
- 82 N. J. Jeon, J. Lee, J. H. Noh, M. K. Nazeeruddin, M. Grätzel and S. I. Seok, *J. Am. Chem. Soc.*, 2013, **135**, 19087–19090.
- 83 C. Huang, W. Fu, C.-Z. Li, Z. Zhang, W. Qiu, M. Shi, P. Heremans, A. K.-Y. Jen and H. Chen, *J. Am. Chem. Soc.*, 2016, **138**, 2528–2531.
- 84 R. Grisorio, R. Iacobellis, A. Listorti, L. De Marco, M. P. Cipolla, M. Manca, A. Rizzo, A. Abate, G. Gigli and G. P. Suranna, *ACS Appl. Mater. Interfaces*, 2017, **9**, 24778–24787.
- 85 K. Rakstys, A. Abate, M. I. Dar, P. Gao, V. Jankauskas, G. n. Jacopin, E. Kamarauskas, S. Kazim, S. Ahmad and M. Grätzel, *J. Am. Chem. Soc.*, 2015, **137**, 16172–16178.
- 86 D. Shinde, J. K. Salunke, N. R. Candeias, F. Tinti, M. Gazzano, P. Wadgaonkar, A. Priimagi, N. Camaioni and P. Vivo, *Sci. Rep.*, 2017, **7**, 46268.
- 87 R. Grisorio, B. Roose, S. Colella, A. Listorti, G. P. Suranna and A. Abate, *ACS Energy Lett.*, 2017, **2**, 1029–1034.
- 88 L. Xuepeng, K. Fantai, G. Rahim, J. Shengli, C. Wangchao, Y. Ting, H. Tasawar, A. Ahmed, G. Fuling, T. Zhan'ao, C. Jian and D. Songyuan, *Energy Technol.*, 2017, **5**, 1788–1794.
- 89 K. Rakstys, S. Paek, M. Sohail, P. Gao, K. T. Cho, P. Gratia, Y. Lee, K. H. Dahmen and M. K. Nazeeruddin, *J. Mater. Chem. A*, 2016, **4**, 18259–18264.
- 90 Z. Iwan, U. M. Javier, G. Paul, A. Juan, G. Giulia, M. O. Agustín, O. Enrique, M. Nazario and N. M. Khaja, *Adv. Energy Mater.*, 2017, **7**, 1601674.
- 91 K. Do, H. Choi, K. Lim, H. Jo, J. W. Cho, M. K. Nazeeruddin and J. Ko, *Chem. Commun.*, 2014, **50**, 10971–10974.
- 92 K. Lim, M.-S. Kang, Y. Myung, J.-H. Seo, P. Banerjee, T. J. Marks and J. Ko, *J. Mater. Chem. A*, 2016, **4**, 1186–1190.
- 93 M. O. Agustín, Z. Iwan, G. B. Inés, G. Paul, R. C. Cristina, A. Sadig, G. Michael, N. M. Khaja and M. Nazario, *Angew. Chem., Int. Ed.*, 2016, **55**, 6270–6274.



- 94 I. García-Benito, I. Zimmermann, J. Urieta-Mora, J. Aragón, A. Molina-Ontoria, E. Orti, N. Martín and M. K. Nazeeruddin, *J. Mater. Chem. A*, 2017, **5**, 8317–8324.
- 95 S. Paek, M. A. Rub, H. Choi, S. A. Kosa, K. A. Alamry, J. W. Cho, P. Gao, J. Ko, A. M. Asiri and M. K. Nazeeruddin, *Nanoscale*, 2016, **8**, 6335–6340.
- 96 R. Kasparas, S. Michael, G. Peng, G. Paul, K. Egidijus, P. Sanghyun, J. Vyngintas and N. M. Khaja, *Angew. Chem., Int. Ed.*, 2016, **55**, 7464–7468.
- 97 W. Ya-Kun, Y. Zhong-Cheng, S. Guo-Zheng, L. Yong-Xi, L. Qian, H. Fei, S. Bao-Quan, J. Zuo-Quan and L. Liang-Sheng, *Adv. Funct. Mater.*, 2016, **26**, 1375–1381.
- 98 R. S. Sudhaker, G. Kumarasamy, H. J. Hyuck, I. S. Hyuk, K. C. Su, K. Dong-Ho, M. J. Hun, L. J. Yong, S. Myungkwan and J. Sung-Ho, *Adv. Mater.*, 2016, **28**, 686–693.
- 99 R. Tiazkis, S. Paek, M. Daskeviciene, T. Malinauskas, M. Saliba, J. Nekrasovas, V. Jankauskas, S. Ahmad, V. Getautis and M. K. Nazeeruddin, *Sci. Rep.*, 2017, **7**, 150.
- 100 D. Bi, B. Xu, P. Gao, L. Sun, M. Grätzel and A. Hagfeldt, *Nano Energy*, 2016, **23**, 138–144.
- 101 B. Xu, J. Zhang, Y. Hua, P. Liu, L. Wang, C. Ruan, Y. Li, G. Boschloo, E. M. Johansson and L. Kloo, *Chem*, 2017, **2**, 676–687.
- 102 T. Malinauskas, M. Saliba, T. Matsui, M. Daskeviciene, S. Urnikaite, P. Gratia, R. Send, H. Wonneberger, I. Bruder and M. Graetzel, *Energy Environ. Sci.*, 2016, **9**, 1681–1686.
- 103 M. Saliba, S. Orlandi, T. Matsui, S. Aghazada, M. Cavazzini, J.-P. Correa-Baena, P. Gao, R. Scopelliti, E. Mosconi and K.-H. Dahmen, *Nat. Energy*, 2016, **1**, 15017.
- 104 W. S. Yang, J. H. Noh, N. J. Jeon, Y. C. Kim, S. Ryu, J. Seo and S. I. Seok, *Science*, 2015, **348**, 1234–1237.
- 105 P. Gratia, A. Magomedov, T. Malinauskas, M. Daskeviciene, A. Abate, S. Ahmad, M. Grätzel, V. Getautis and M. K. Nazeeruddin, *Angew. Chem., Int. Ed.*, 2015, **54**, 11409–11413.
- 106 T. Leijtens, T. Giovenzana, S. N. Habisreutinger, J. S. Tinkham, N. K. Noel, B. A. Kamino, G. Sadoughi, A. Sellinger and H. J. Snaith, *ACS Appl. Mater. Interfaces*, 2016, **8**, 5981–5989.
- 107 S. D. Sung, M. S. Kang, I. T. Choi, H. M. Kim, H. Kim, M. Hong, H. K. Kim and W. I. Lee, *Chem. Commun.*, 2014, **50**, 14161–14163.
- 108 J. Wang, Y. Chen, F. Li, X. Zong, J. Guo, Z. Sun and S. Xue, *Electrochim. Acta*, 2016, **210**, 673–680.
- 109 M. S. Kang, S. D. Sung, I. T. Choi, H. Kim, M. Hong, J. Kim, W. I. Lee and H. K. Kim, *ACS Appl. Mater. Interfaces*, 2015, **7**, 22213–22217.
- 110 M. Daskeviciene, S. Paek, Z. Wang, T. Malinauskas, G. Jokubauskaite, K. Rakstys, K. T. Cho, A. Magomedov, V. Jankauskas and S. Ahmad, *Nano Energy*, 2017, **32**, 551–557.
- 111 C. Zhiliang, L. Hui, Z. Xiaolu, Z. Qi, L. Zhanfeng, H. Yuying and F. Guojia, *ChemSusChem*, 2017, **10**, 3111–3117.
- 112 Z. Hongwei, Z. Fei, L. Xicheng, S. Mengna, H. Jianlei, Y. Jing, W. Shirong, X. Yin and L. Xianggao, *Energy Technol.*, 2017, **5**, 1257–1264.
- 113 Z. Linna, S. Yahan, W. Rui, L. Debei, Z. Cheng, S. Qunliang and W. Fei, *Chem.–Eur. J.*, 2017, **23**, 4373–4379.
- 114 X. Bo, S. Esmaeil, L. Peng, Z. Jinbao, T. Haining, V. Nick, B. Gerrit, K. Lars, H. Anders and S. Licheng, *Adv. Mater.*, 2014, **26**, 6629–6634.
- 115 H. Wang, A. D. Sheikh, Q. Feng, F. Li, Y. Chen, W. Yu, E. Alarousu, C. Ma, M. A. Haque and D. Shi, *ACS Photonics*, 2015, **2**, 849–855.
- 116 F. Di Giacomo, S. Razza, F. Matteocci, A. D'Epifanio, S. Licoccia, T. M. Brown and A. Di Carlo, *J. Power Sources*, 2014, **251**, 152–156.
- 117 E. Gabrielsson, H. Ellis, S. Feldt, H. Tian, G. Boschloo, A. Hagfeldt and L. Sun, *Adv. Energy Mater.*, 2013, **3**, 1647–1656.
- 118 F. Wu, Y. Ji, R. Wang, Y. Shan and L. Zhu, *Dyes Pigm.*, 2017, **143**, 356–360.
- 119 X. Li, M. Cai, Z. Zhou, K. Yun, F. Xie, Z. Lan, J. Hua and L. Han, *J. Mater. Chem. A*, 2017, **5**, 10480–10485.
- 120 M. Petrus, T. Bein, T. Dingemans and P. Docampo, *J. Mater. Chem. A*, 2015, **3**, 12159–12162.
- 121 W. S. Yang, B.-W. Park, E. H. Jung, N. J. Jeon, Y. C. Kim, D. U. Lee, S. S. Shin, J. Seo, E. K. Kim and J. H. Noh, *Science*, 2017, **356**, 1376–1379.
- 122 X. Zheng, B. Chen, J. Dai, Y. Fang, Y. Bai, Y. Lin, H. Wei, X. C. Zeng and J. Huang, *Nat. Energy*, 2017, **2**, 17102.
- 123 Z. Zhuang, Y. Li, D. Qi, C. Zhao and H. Na, *Sens. Actuators, B*, 2017, **242**, 801–809.
- 124 W. Ma, C. Yang, X. Gong, K. Lee and A. J. Heeger, *Adv. Funct. Mater.*, 2005, **15**, 1617–1622.
- 125 H. Yoon, S. M. Kang, J.-K. Lee and M. Choi, *Energy Environ. Sci.*, 2016, **9**, 2262–2266.
- 126 L. Kyung-Geun, A. Soyeong, K. Hobeom, C. Mi-Ri, H. D. Ho and L. Tae-Woo, *Adv. Mater. Interfaces*, 2016, **3**, 1500678.
- 127 K.-G. Lim, S. Ahn, Y.-H. Kim, Y. Qi and T.-W. Lee, *Energy Environ. Sci.*, 2016, **9**, 932–939.
- 128 K. G. Lim, H. B. Kim, J. Jeong, H. Kim, J. Y. Kim and T. W. Lee, *Adv. Mater.*, 2014, **26**, 6461–6466.
- 129 A. Dubey, N. Adhikari, S. Venkatesan, S. Gu, D. Khatriwada, Q. Wang, L. Mohammad, M. Kumar and Q. Qiao, *Sol. Energy Mater. Sol. Cells*, 2016, **145**, 193–199.
- 130 M. Wong-Stringer, J. E. Bishop, J. A. Smith, D. K. Mohamad, A. J. Parnell, V. Kumar, C. Rodenburg and D. G. Lidzey, *J. Mater. Chem. A*, 2017, **5**, 15714–15723.
- 131 Z. Yu, Y. Zhang, X. Jiang, X. Li, J. Lai, M. Hu, M. Elawad, G. G. Gurzadyan, X. Yang and L. Sun, *RSC Adv.*, 2017, **7**, 27189–27197.
- 132 Z. Zhou, Y. Zhao, C. Zhang, D. Zou, Y. Chen, Z. Lin, H. Zhen and Q. Ling, *J. Mater. Chem. A*, 2017, **5**, 6613–6621.
- 133 J. Liu, Q. Ge, W. Zhang, J. Ma, J. Ding, G. Yu and J. Hu, *Nano Res.*, 2018, **11**, 185–194.
- 134 E. A. Gaml, A. Dubey, K. M. Reza, M. N. Hasan, N. Adhikari, H. Elbohy, B. Bahrami, H. Zeyada, S. Yang and Q. Qiao, *Sol. Energy Mater. Sol. Cells*, 2017, **168**, 8–13.



- 135 K. Rakstys, S. Paek, P. Gao, P. Gratia, T. Marszalek, G. Grancini, K. T. Cho, K. Genevicius, V. Jankauskas and W. Pisula, *J. Mater. Chem. A*, 2017, **5**, 7811–7815.
- 136 J. H. Heo, S. Park, S. H. Im and H. J. Son, *ACS Appl. Mater. Interfaces*, 2017, **9**, 39511–39518.
- 137 J. Lee, M. Malekshahi Byranvand, G. Kang, S. Y. Son, S. Song, G.-W. Kim and T. Park, *J. Am. Chem. Soc.*, 2017, **139**, 12175–12181.
- 138 A. S. Subbiah, A. Halder, S. Ghosh, N. Mahuli, G. Hodes and S. K. Sarkar, *J. Phys. Chem. Lett.*, 2014, **5**, 1748–1753.
- 139 K.-C. Wang, P.-S. Shen, M.-H. Li, S. Chen, M.-W. Lin, P. Chen and T.-F. Guo, *ACS Appl. Mater. Interfaces*, 2014, **6**, 11851–11858.
- 140 Z. Liu, A. Zhu, F. Cai, L. Tao, Y. Zhou, Z. Zhao, Q. Chen, Y.-B. Cheng and H. Zhou, *J. Mater. Chem. A*, 2017, **5**, 6597–6605.
- 141 P. H. Duc, W. Zhifang, L. K. Ono, M. Sergei, F. Krishna, M. Nunzio, Q. Yabing and S. Prashant, *Adv. Electron. Mater.*, 2017, **3**, 1700139.
- 142 J. A. Christians, R. C. Fung and P. V. Kamat, *J. Am. Chem. Soc.*, 2013, **136**, 758–764.
- 143 B. A. Nejand, V. Ahmadi, S. Gharibzadeh and H. R. Shahverdi, *ChemSusChem*, 2016, **9**, 302–313.
- 144 Y. Wang, Z. Xia, J. Liang, X. Wang, Y. Liu, C. Liu, S. Zhang and H. Zhou, *Semicond. Sci. Technol.*, 2015, **30**, 054004.
- 145 P. Qin, S. Tanaka, S. Ito, N. Tetreault, K. Manabe, H. Nishino, M. K. Nazeeruddin and M. Grätzel, *Nat. Commun.*, 2014, **5**, 3834.
- 146 V. E. Madhavan, I. Zimmermann, C. Roldán-Carmona, G. Grancini, M. Buffiere, A. Belaidi and M. K. Nazeeruddin, *ACS Energy Lett.*, 2016, **1**, 1112–1117.
- 147 Y. S. Kwon, J. Lim, H.-J. Yun, Y.-H. Kim and T. Park, *Energy Environ. Sci.*, 2014, **7**, 1454–1460.
- 148 X. Liang, C. Wang, M. Wu, Y. Wu, F. Zhang, Z. Han, X. Lu, K. Guo and Y.-M. Zhao, *Tetrahedron*, 2017, **73**, 7115–7121.
- 149 F. Xie, C.-C. Chen, Y. Wu, X. Li, M. Cai, X. Liu, X. Yang and L. Han, *Energy Environ. Sci.*, 2017, **10**, 1942–1949.
- 150 H. Li, K. Fu, A. Hagfeldt, M. Grätzel, S. G. Mhaisalkar and A. C. Grimsdale, *Angew. Chem., Int. Ed.*, 2014, **53**, 4085–4088.
- 151 C. Laura, K. Samrana, G. Michael and A. Shahzada, *Angew. Chem., Int. Ed.*, 2016, **55**, 14522–14545.
- 152 Y. Ze and S. Licheng, *Adv. Energy Mater.*, 2015, **5**, 1500213.
- 153 Z. H. Bakr, Q. Wali, A. Fakharuddin, L. Schmidt-Mende, T. M. Brown and R. Jose, *Nano Energy*, 2017, **34**, 271–305.
- 154 L. Etgar, P. Gao, Z. Xue, Q. Peng, A. K. Chandiran, B. Liu, M. K. Nazeeruddin and M. Grätzel, *J. Am. Chem. Soc.*, 2012, **134**, 17396–17399.
- 155 S. Aharon, S. Gamliel, B. El Cohen and L. Etgar, *Phys. Chem. Chem. Phys.*, 2014, **16**, 10512–10518.
- 156 Z. Ku, Y. Rong, M. Xu, T. Liu and H. Han, *Sci. Rep.*, 2013, **3**, 3132.
- 157 J. Xu, O. Voznyy, R. Comin, X. Gong, G. Walters, M. Liu, P. Kanjanaboos, X. Lan and E. H. Sargent, *Adv. Mater.*, 2016, **28**, 2807–2815.
- 158 N. K. Elumalai, M. A. Mahmud, D. Wang and A. Uddin, *Energies*, 2016, **9**, 861.
- 159 D. A. Egger, E. Edri, D. Cahen and G. Hodes, *J. Phys. Chem. Lett.*, 2015, **6**, 279–282.
- 160 W. Tress, N. Marinova, T. Moehl, S. M. Zakeeruddin, M. K. Nazeeruddin and M. Grätzel, *Energy Environ. Sci.*, 2015, **8**, 995–1004.
- 161 J. Wei, Y. Zhao, H. Li, G. Li, J. Pan, D. Xu, Q. Zhao and D. Yu, *J. Phys. Chem. Lett.*, 2014, **5**, 3937–3945.
- 162 H.-W. Chen, N. Sakai, M. Ikegami and T. Miyasaka, *J. Phys. Chem. Lett.*, 2014, **6**, 164–169.
- 163 J. M. Frost, K. T. Butler, F. Brivio, C. H. Hendon, M. Van Schilfgaarde and A. Walsh, *Nano Lett.*, 2014, **14**, 2584–2590.
- 164 R. S. Sanchez, V. Gonzalez-Pedro, J.-W. Lee, N.-G. Park, Y. S. Kang, I. Mora-Sero and J. Bisquert, *J. Phys. Chem. Lett.*, 2014, **5**, 2357–2363.
- 165 O. Almora, I. Zarazua, E. Mas-Marza, I. Mora-Sero, J. Bisquert and G. Garcia-Belmonte, *J. Phys. Chem. Lett.*, 2015, **6**, 1645–1652.
- 166 A. Krishna and A. C. Grimsdale, *J. Mater. Chem. A*, 2017, **5**, 16446–16466.
- 167 Z. Meng, L. Miaoqiang, Y. Hua, Y. Jung-Ho, W. Qiong and W. Lianzhou, *Chem.-Eur. J.*, 2015, **21**, 434–439.
- 168 Y. Xiao, G. Han, Y. Chang, H. Zhou, M. Li and Y. Li, *J. Power Sources*, 2014, **267**, 1–8.

